Materials Science & Engineering C 102 (2019) 373–390

Contents lists available at ScienceDirect

Materials Science & Engineering C

journal homepage: www.elsevier.com/locate/msec

Cold-adaptation of a methacrylamide gelatin towards the expansion of the biomaterial toolbox for specialized functionalities in tissue engineering

Alessandro Zaupa[a,e], Nicholas Byres[a,b,d], Chiara Dal Zovo[a], Cristian A. Acevedo[h,i], Ioannis Angelopoulos[a,b], Claudia Terraza[a,b], Nikolaus Nestle[g], Phammela N. Abarzúa-Illanes[a], Franck Quero[j], Paulo Díaz-Calderón[e], Yusser Olguín[k], Tamara L. Akentjew[a,n], Camila A. Wilkens[a], Cristina Padilla[e], Flavia C. Zacconi[m], Karina Pino-Lagos[l], Jonny J. Blaker[c,d], Maroun Khoury[a,b,f], Javier Enrione[e], Juan Pablo Acevedo[a,b,f,*]

[a] Laboratory of Nano-Regenerative Medicine, Faculty of Medicine, Universidad de los Andes, Santiago, Chile
[b] Cells for Cells, Santiago, Chile
[c] Bio-Active Materials Group, School of Materials, MSS Tower, The University of Manchester, Manchester M13 9PL, UK
[d] School of Materials, MSS Tower, The University of Manchester, Manchester M13 9PL, UK
[e] Biopolymer Research and Engineering Lab (BiopREL), School of Nutrition and Dietetics, Faculty of Medicine, Universidad de los Andes, Santiago, Chile
[f] Consorcio Regenero, Santiago, Chile
[g] BASF SE Advanced Materials and Systems Research, D-67056 Ludwigshafen, Germany
[h] Centro de Biotecnología, Universidad Técnica Federico Santa María, Avenida España 1680, Valparaíso 2340000, Chile
[i] Departamento de Física, Universidad Técnica Federico Santa María, Avenida España 1680, Valparaíso 2340000, Chile
[j] Laboratorio de Nanocelulosa y Biomateriales, Departamento de Ingeniería Química, Biotecnología y Materiales, Facultad de Ciencias Físicas y Matemáticas, Universidad de Chile, Avenida Beauchef 851, Santiago, Chile
[k] Centro Científico Tecnológico de Valparaíso (CCTVal), Universidad Técnica Federico Santa María, Avenida España 1680, Valparaíso, Chile
[l] Centro de Investigación Biomédica, Facultad de Medicina, Universidad de los Andes, Santiago, Chile
[m] Departamento de Química Orgánica, Facultad de Química, Pontificia Universidad Católica de Chile, Vicuña Mackenna 4860, Macul, 78204336, Santiago, Chile
[n] Department of Chemical and Bioprocess Engineering, School of Engineering, Pontificia Universidad Católica de Chile, Santiago, Chile

ARTICLE INFO

Keywords:
Cold-adapted
Gelatin
Salmon
Methacrylamide
Tissue engineering

ABSTRACT

Tissue regeneration is witnessing a significant surge in advanced medicine. It requires the interaction of scaffolds with different cell types for efficient tissue formation post-implantation. The presence of tissue subtypes in more complex organs demands the co-existence of different biomaterials showing different hydrolysis rate for specialized cell-dependent remodeling. To expand the available toolbox of biomaterials with sufficient mechanical strength and variable rate of enzymatic degradation, a cold-adapted methacrylamide gelatin was developed from salmon skin. Compared with mammalian methacrylamide gelatin (GelMA), hydrogels derived from salmon GelMA displayed similar mechanical properties than the former. Nevertheless, salmon gelatin and salmon GelMA-derived hydrogels presented characteristics common of cold-adaptation, such as reduced activation energy for collagenase, increased enzymatic hydrolysis turnover of hydrogels, increased interconnected polypeptides molecular mobility and lower physical gelation capability. These properties resulted in increased cell-remodeling rate *in vitro* and *in vivo*, proving the potential and biological tolerance of this mechanically adequate cold-adapted biomaterial as alternative scaffold subtypes with improved cell invasion and tissue fusion capacity.

* Corresponding author at: Laboratory of Nano-Regenerative Medicine, Faculty of Medicine, Universidad de los Andes, Av. Plaza 2500, Las Condes, Santiago, Chile.
E-mail addresses: alessandro.zaupa@gmail.com (A. Zaupa), nicholas.byres@manchester.ac.uk (N. Byres), chiaradz@gmail.com (C. Dal Zovo), cristian.acevedo@usm.cl (C.A. Acevedo), iangelopoulos@uandes.cl (I. Angelopoulos), cterraza@c4c.cl (C. Terraza), nikolaus.nestle@basf.com (N. Nestle), pabarzua@uandes.cl (P.N. Abarzúa-Illanes), fquero@ing.uchile.cl (F. Quero), pdiaz@uandes.cl (P. Díaz-Calderón), yusser.olguin@postgrado.usm.cl (Y. Olguín), tlakentj@uc.cl (T.L. Akentjew), camiwhy@gmail.com (C.A. Wilkens), cpadilla@uandes.cl (C. Padilla), fzacconi@uc.cl (F.C. Zacconi), kpino@uandes.cl (K. Pino-Lagos), jonny.blaker@manchester.ac.uk (J.J. Blaker), mkhoury@uandes.cl (M. Khoury), jenrione@uandes.cl (J. Enrione), jpacevedo@uandes.cl (J.P. Acevedo).

https://doi.org/10.1016/j.msec.2019.04.020
Received 11 September 2018; Received in revised form 28 March 2019; Accepted 8 April 2019
Available online 12 April 2019
0928-4931/

1. Introduction

The use of specialized polymeric scaffolds is often applied to several approaches in the field of regenerative medicine and tissue engineering [1]. Scaffolds, either alone [2] or in combination with cells [3], have proven potential to induce regenerative processes and to assist the formation of new functional tissues [4,5]. Successful tissue integration with the scaffold requires the orchestration of several cellular activities, including infiltration, proliferation, differentiation and scaffold remodeling, which are performed in conjunction by different cell types to regenerate functional and appropriately vascularized tissues [6]. These individual events could be affected and disrupted by the nature of the scaffold material, 3D structural organization and the specific interaction between the material and the different type of cells. Therefore, and in addition to the understanding of these processes [7], scientists need access to a broader toolbox of available materials to efficiently orchestrate the tissue integration processes to give functional and well-structured tissues after implantation.

Unlike biomaterials based on natural polymers, synthetic polymers typically do not support cell adhesion, and cannot undergo cell-dependent hydrolytic degradation and remodeling [8,9], unless non-specified protein adsorption occurs, or stimulatory cues are tethered to the synthetic polymer [10]. In the spectrum of natural biomaterials, many polysaccharides such as alginate, cellulose, chitosan and agarose cannot undergo cell-active degradation due to the lack of specialized enzymes in mammalian systems, becoming a major barrier for tissue fusion [11,12].

Gelatin is a water-soluble biomaterial obtained after inexpensive extraction processes from collagen-containing waste streams/by-products from meat, poultry and fish industries, in which the natural extracellular matrix (ECM) is submitted to partial hydrolysis and denaturation. Gelatin retains motifs for cell attachment and cell-active remodeling [13], serving as a suitable material for scaffolds fabrication. Contrary to collagen, gelatin solutions derived from bovine and porcine, can be (reversibly) thermally activated to triple helix conformation (gelation or physical crosslinking) at ~25 °C, or random coil (liquid state) at physiological temperatures (37 °C) [14], limiting its use in mammalian models. This constraint has been predominantly overcome by adding functional groups on lysine side chains, which can be covalently crosslinked to other adjacent functional groups [15]. Gelatin can be functionalized with methacrylamide groups, commonly termed methacrylamide gelatin (GelMA), and can form water-insoluble hydrogels under physiological conditions through free radical polymerization induced by a photoinitiator and light, by suitable thermal initiator or by chemical initiator [16]. This avoids structural disruption that usually occurs at 37 °C for non-functionalized gelatin.

Photo-crosslinkable bovine and porcine gelatin have been extensively used in research, showing suitable mechanical properties and bioactivity for tissue engineering and regenerative applications. This means that cells can survive, proliferate and execute appropriated cellular function in presence or embedded within this biomaterial [17–19]. Non-mammalian collagen such as salmon collagen has also been proposed as biomaterial for tissue engineering, and exhibits improved elastic properties for chemically crosslinked collagen, good cell attachment and proliferation [20] and adequate hemocompatibility [21]. Moreover, a recent work demonstrated that methacrylamide functionalization and photo-crosslinking of hydrolyzed skin-derived gelatin from (undefined) cold-water fishes, could expand the use of crosslinked gelatin to a wider range of potential applications in tissue engineering due to its lower sol-gel transition and higher enzymatic degradability compared to porcine GelMA. However, lower mechanical toughness was measured for this material, limiting the usability in application where compression or tensile strength is a concern [22]. On the other hand, the use of this gelatin source in regenerative medicine is of particular relevance in diverse societies and regulatory policies. It can obviate religious, cultural and/or disease transmission implications that otherwise can arise from the use of gelatin from mammalian origin [23].

A distinctive feature of gelatin from cold-adapted organisms, such as salmon, is their intrinsic molecular mobility at lower temperatures when compared with gelatin extracted from mammalian organisms. This has been explained by the lower number of proline and hydroxyproline in the amino acid sequence and average molecular weight of salmon gelatin compared to mammalian gelatin [24,25]. Previous thermodynamic evidence on peptidases (EC3.4 enzymes) [26,27] leads one to presume that higher molecular mobility of salmon gelatin could enhance the catalytic efficiency of collagenases and metalloproteinases (MMPs), mainly due to their lower enthalpic requirement to reach the point of higher potential energy (transition state) necessary for the biocatalytic reaction [26,27]. This feature could imbue an improvement in cell migration/invasion, angiogenesis and tissue integration of scaffolds *in vivo*, possibly at the expense of impaired mechanical properties as reported in a previous study [22].

In order to reveal the bases of improvement and the potential usability of salmon gelatin as a cold-adapted biomaterial for tissue engineering applications, this work explored the molecular nature and biological characteristics of salmon GelMA hydrogels through a comprehensive series of *in vitro* experiments, benchmarking it with bovine GelMA hydrogels. Here, our findings describe an increased protease catalytic efficiency over flexible cold-adapted gelatin polypeptide and improved turnover of peptidases over hydrogels based on salmon GelMA, this as a result of higher molecular mobility. Strikingly, hydrogels of salmon GelMA showed similar Young's modulus compared with hydrogels based on bovine GelMA, but improved capacity of cell-remodeling *in vitro* and *in vivo*.

2. Materials and methods

2.1. Fabricacion of methacrylamide bovine and salmon gelatin

Salmon gelatin (SG) was first extracted from the skins of atlantic salmon (*Salmo salar*) following the methodology previously reported [25]. Manually de-fleshed salmon skins were cut into 2 cm^2 squares and subjected to basic pretreatment in NaOH 0.1 M solution at 10 °C under mechanical agitation for 1 h (6 ml/g of skin). After washing in deionized water (dH_2O), skin pieces were treated again under the same conditions. Afterward, skin pieces were further washed in abundant dH_2O, filtered to remove excess water and treated with a solution of acetic acid 0.05 M (6 ml/g of skin) at 10 °C for 1 h under continuous overhead agitation. Prior to acidic extraction, skin pieces were extensively rinsed with dH_2O and submerged in dH_2O (6 ml/g of skin), adjusting the pH to 4.0 by adding a controlled amount of acetic acid dropwise. The acidic extraction was performed for 4 h under continuous overhead agitation at 60 °C. After extraction, any large skin fragments were discarded after vacuum filtration of the product using 20 μm pore filter paper and subsequently dried in an oven at 50 °C for 48 h. The resultant gelatin films were grounded, hermetically sealed under vacuum and stored at room temperature (20 °C) until further use.

Chemical functionalization of the above-described extracted salmon gelatin and commercial bovine gelatin (BG) (comparative control, Bloom 220, Rousselot, Netherlands) with methacrylamide groups was performed by reacting methacrylic anhydride (MAA) (#276685, Sigma) with the free amino groups of the gelatins as previously reported for porcine and bovine gelatin [17,28]. Briefly, salmon and bovine gelatin were dissolved to a concentration of 10% (w/v) in PBS 1× (pH 7.4) at 60 °C. After complete dissolution, methacrylic anhydride (#276685, Sigma, USA) was added dropwise to final concentrations of 0.5%, 2%, 5%, 8% or 10% (v/v) under continuous stirring and incubated for 3 h at 60 °C, without controlling pH during the reaction. These GelMA preparations are named using the three terms nomenclature that describe the species source, amount of methacrylic anhydride used during functionalization and the “M” that stand for “methacrylamide” (*e.g.*

S2M, B5M). The different concentrations of methacrylic anhydride were applied in order to obtain different degree of functionalization for salmon and bovine gelatin. The reaction was terminated by adding 3 volumes of PBS 1× and by dialyzing (12 kDa MWCO dialysis bags, D9527, Sigma, USA) against dH_2O (1.10) at 40 °C for 1 week with dH_2O replaced twice daily (conductivity and pH was measured to ensure dialysis completion). Finally, the dialyzed mixture was freeze dried and kept at −20 °C until further use.

2.2. Amino acid composition

To determine or discard differences in amino acid composition due to functionalization, only salmon and bovine gelatin that reacted with high concentration of MAA (2%, 5%, 10% v/v) were used for analysis and compared to non-functionalized gelatins. A study of amino acid composition was carried out following the methodology previously described [25,29,30], using high-performance liquid chromatography (HPLC). Briefly, 10 mg of the samples were hydrolyzed under acidic conditions during 24 h with 6 N HCl, phenol 1% (v/v) at 110 °C. The hydrolysate was dried at vacuum and re-suspended in 20 µl of ethanol/water/triethylamine (1:1:1), preceding a second vacuum drying step. In order to perform derivatization of amino acids into phenylthiocarbamyl amino acids, 20 µl of ethanol/water/trimethylamine/phenylisothiocyanate (7:1:2:1) was added and incubated for 10 min at room temperature and dried again. Phenylthiocarbamyl amino acids were separated in a HPLC Waters 600 controller (Massachusets, USA) coupled to a diode array detector Waters 996 using an RP 18 column (Phenomenex Luna, Los Angeles, California). The separation gradient was constituted using a 0.14 M anhydrous sodium acetate (pH 5.9)/acetonitrile (94:6) solution and an acetonitrile/water (60:40) solution. The column temperature was set at 40 °C. Amino acid determination was performed using commercial amino acid standards (Sigma-Aldrich, Steinheim, Germany). During the hydrolysis step, yields for serine, threonine and tyrosine are found to be 90%, 94% and 97% respectively. Glutamine and asparagine concentrations could not be distinguished from glutamate and aspartate, both respectively.

2.3. Hydrolysis degree assessment of extracted gelatin

To validate that both salmon and bovine gelatin are comparable in terms of degree of hydrolysis, sodium dodecyl sulfate-polyacrylamide gel electrophoresis (SDS-PAGE) qualitative analysis, lysine composition and quantitative estimation of free aminos was performed. Classical determination of molecular weight by SDS-PAGE was performed as previously described [31], and used qualitatively to observe the molecular weight range and dispersion of hydrolyzed polypeptides. Determination of lysine content was calculated from the whole amino acid composition analysis explained previously and expressed as mmol/100 g of gelatin. Finally, the number of α-amino groups from the NH_2-terminal polypeptide and free ε-amino groups of lysine was indistinctly quantified using the o-phthaldialdehyde (OPA) method [32]. Briefly, 100 ml of OPA solution was prepared dissolving 3.81 g of di-Na-tetraborate decahydrate (Sigma, USA) and 100 mg Na-dodecyl-sulfate (SDS) (Sigma, USA) in 75 ml of dH_2O. Afterwards, 88 mg of dithiothreitol 99% (DTT) (Sigma, USA) re-suspended in 2 ml of ethanol was added to the solution and completed to 100 ml with dH_2O. GelMA gelatins and control gelatin solutions were prepared at a concentration of 20 mg/ml in dH_2O. Afterwards, 3 ml of OPA solution were mixed with 400 µl of the gelatin sample, incubated for 2 min and the absorbance measured at 340 nm using a plate reader (Infinite 200 PRO, TECAN, Switzerland). A standard curve for primary amines was fabricated using different concentrations of serine amino acid (0.1–0.03 mg/ml) (Sigma, USA). dH_2O was used as the blank sample and non-functionalized salmon and bovine gelatin as the controls for 0% degree of functionalized primary amino groups.

2.4. Quantification of the degree of methacrylamide functionalization

Two complementary methodologies were applied to provide an estimation of the degree of functionalization of lysine in the GelMA samples, later used to define percentage of methacrylamide lysines from the total lysines present in the respective gelatins. The OPA method was first used to quantify the percentage of free ε-amino groups of lysine that did not react with the methacrylic anhydride [32]. OPA reacts with free primary amines, including α-amino groups from the NH_2-terminal polypeptide and free ε-amino groups of lysine, therefore, providing that the hydrolysis degree between two samples is similar (equivalent number of NH_2-terminal polypeptide), this OPA method would be reliable to quantify comparatively the degree of lysine functionalization of different gelatin samples [33].

^{1}H NMR spectroscopy was applied as a corollary technique to determine the ratio between methacrylamide lysine in the functionalized samples to lysine in the non-functionalized gelatins. [34] Briefly, gelatin samples were prepared by dissolving 10 mg of lyophilized gelatins in deuterium oxide (D_2O) and analyzed using high-resolution 500 MHz proton NMR spectra (Bruker Avance 500 spectrometer, Ettlingen, Germany). For comparative quantification, spectra normalization was performed using the phenylalanine signal (6.9–7.5 ppm, “I” peak in the spectra). Lysine methylene signals are situated at 2.8–2.95 ppm, (“II” peak in the spectra) and the area under the curve for the GelMA samples (A(PII)GelMA) and non-functionalized gelatin samples (A(PII)Gelatin) were used to calculate the percentage of functionalized lysine (F %) in every GelMA sample using the equation

$$F\% = \left(\frac{1 - \mathrm{A(PII)GelMA}}{\mathrm{A(PII)Gelatin}}\right) \times 100 \quad (1)$$

Additional signals (5.4, 5.7, 6.1 ppm) were also considered to assess whether possible additional functionalization at hydroxyl groups in the gelatin occurred.

2.5. Isoelectric point and zeta potential determination

The isoelectric points of salmon and bovine gelatin samples at different degree of functionalization were obtained via zeta-potential measurement at different pH in a solution of 0.1 M of NaCl using a Zetasizer Nano ZS 90 (Malvern Instruments, Worcestershire, UK). pH titration was conducted using a Autotritator MPT-2 (Malvern Instruments, Worcestershire, UK) loaded with 3 titrant solutions (NaOH 0.1 M, HCl 0.1 M and HCl 0.01 M), which allowed a controlled pH adjustment of the solution. Samples were prepared at a concentration of 1.5 g/l after dissolution for 60 min at 50 °C. Zeta potentials were measured at 40 °C over a pH titration in the range of 2–12, with 0.1 pH steps. The pH at which the zeta potential is 0 mV was defined as the isoelectric point of the gelatin sample [35], and the zeta potential at pH 7.4 (physiological condition) was used as a subrogated value of surface charges present of the gelatins in solution.

2.6. Differential scanning calorimetry (DSC)

The melting points of gelated gelatin solutions were determined using differential scanning calorimetry (DSC) (Mettler Toledo, Switzerland). Samples of ~20 mg in weight having total volume of 40 µl in dH_2O were hermetically sealed in aluminum pans. The samples were annealed for 1 h at 1 °C prior to thermal scanning, and subsequently heated at 1 °C/min from 1 °C up to 30 °C (salmon) or up to 60 °C (bovine). The DSC was previously calibrated using indium as a standard and an empty pan was used as reference under a 40-ml/min-nitrogen flow. The melting temperature (T_m) was determined as the onset of the endothermic peak observed upon heating. The enthalpy of melting (ΔH_m) was calculated as the area of the endothermic peak. The endothermic transition width (ΔT) was estimated as the difference

between the onset and offset temperatures. A two-level full factorial experiment (with center point per triplicate) was used to evaluate the melting behavior of salmon-derived GelMA samples as a function of concentration, degree of functionalization and interaction between these two variables. The estimation of significance of variables and their interaction was performed using the software MODDE (Umetrics, Sweden).

2.7. Gelatin crosslinking

Hydrogels were fabricated by free radical polymerization of a solution of methacrylamide gelatin (or GelMA) exposed to UV light. To undergo free radical polymerization of GelMA in solution, a photoinitiator (PI) was used to a final concentration of 0.2% (w/v). A 5% (w/v) PI stock solution was prepared from 2-hydroxy-4′-(2-hydroxyethoxy)-2-methylpropiophenone (410896, Sigma, USA; also known as Irgacure 2959) in a solution of PBS 1× by heating at 70 °C and kept under stirring until complete dissolution. A 20% (w/v) stock solution of GelMA (salmon or bovine) was prepared in PBS 1× by stirred incubation at 37 °C for 5 h. All solutions were freshly prepared for each experiment and the base formulation consisted of 7–10% (w/v) GelMA and 0.2% (w/v) PI in PBS 1× (pH 7.4). These solutions were then poured in PDMS molds (Ellsworth, USA), 10 mm in diameter and 3.14 mm in height unless stated otherwise and covered with PDMS caps. Gelatin crosslinking and hydrogel formation was achieved after exposing the base formulation to UV light filtered to 365 nm. with an intensity of 261 mW/cm^2 (OmniCure® S2000, Excelitas Technologies, USA) at a distance of 10 cm for 2 min or 30 s if cells were present. UV intensity was checked for every experiment using a radiometer (R2000, Omnicure®, USA) through a covering material in case photo-crosslinking of solution is performed in covered molds. It is important to remark that GelMA photo-crosslinking within a gas permeable PDMS mold generated a thin uncured layer (approximately 50 μm in thickness) at the interface between the PDMS and the hydrogel under formation, known as the oxygen-containing “dead zone” [36]. Considering the 10 mm in diameter and 3.14 mm in height of the PDMS mold, and that the whole study used identical molding conditions, the possible existence of the uncured layer surrounding the GelMA hydrogel was ignored in this study. On the other hand, although the dissolved oxygen in GelMA solution could inhibit the photo-crosslinking reaction under certain conditions, the chosen UV intensity and time of exposure guaranteed an appropriate and standard level of polymerization completion [37].

2.8. Mechanical testing for non-induced and induced triple helix photo-crosslinking hydrogels

Cylindrical photo-crosslinked hydrogels, strictly identical in size, were fabricated as described earlier. More in detail, for non-induced triple helix hydrogels, the base formulation of functionalized gelatins were carefully pre-warmed at 40 °C and poured into PDMS molds, which were also kept at 40 °C in an incubator. UV photo-crosslinking was performed within the incubator at 40 °C to maintain stable random coil configuration of polypeptides throughout the process. Mechanical testing of the cylindrical hydrogels was performed by dynamic mechanical analysis (using a DMA 1, Mettler Toledo, USA) in compression mode, to enable determination of compressive modulus. In all DMA tests, specimens were subjected to isothermal (25 °C) oscillatory compression at a frequency of 1 Hz with incremental deformation from 1 to 50 μm, with increasing oscillatory increments of 2 μm. Analyses were performed at the linear section of the deformation curve. Complementary to this, tensile test were performed on a mechanical tester (TA.XTplus, Stable Micro Systems Ltd., UK). Hydrogels were fabricated as described before in this section, using PDMS fabricated molds to resemble the standard tensile test specimen conformation for microtensile analysis (“dogbone” shaped hydrogel, 3.8 cm in length, 0.6 cm in width and 0.3 cm in height). To calculate the Young's modulus, tensile tests were conducted using a rate of deformation of 0.2 mm s^{-1}, to 75% strain. The Young's modulus was calculated from the slope of the stress/strain curve that included data to 4% strain.

For induced triple helix photo-crosslinked hydrogels, compression tests were carried out identically to the aforementioned compression testing by DMA, with the distinction that the samples were subjected to a 2 h period of undercooling at 4 °C before photo-crosslinking took place. During the undercooling period the sample molds were sealed with a PDMS lid to stop moisture loss; this technique was confirmed by weighing the samples before and after the undercooling period. Four replicates per sample type were assessed, averages and their associated standard deviations are reported.

2.9. ^{1}H NMR relaxation

Cylindrical gelatin-based hydrogels having various crosslinking degrees were prepared using GelMA base formulation at 7% (w/v) gelatin concentration. Hydrogels were fabricated as described earlier, except that PBS 1× had to be replaced by dH_2O. The samples were allowed to swell to equilibrium by keeping them in dH_2O for 1 week at 4 °C. Prior to NMR measurements, excess surface water was carefully removed from hydrogels using paper tissue. The hydrogels were subsequently inserted into 1 cm diameter NMR tubes. Measurements were conducted at 30 °C in a Bruker minispec mq20 TD-NMR spectrometer (proton resonance frequency 20 MHz) using a solid-echo (SE) CPMG ^{1}H NMR sequence. Transverse or spin-spin relaxation times T_2 were determined from the echo decay curves using multicomponent fitting with a triexponential model described by the equation

$$M(t) = p_{e1}\exp\left(-\frac{t}{T_{2e1}}\right) + p_{e2}\exp\left(-\frac{t}{T_{2e2}}\right) + p_{e3}\exp\left(-\frac{t}{T_{2e3}}\right) \quad (2)$$

where p_{e1} represents the signal from the polymer fraction, while p_{e2} and p_{e3} correspond to the signal from different water populations contained in the sample.

The average relaxation rate of the water phase was calculated with the equation

$$\frac{1}{T_{2\,water}} = \frac{p_{e2}}{T_{2e2}} + \frac{p_{e3}}{T_{2e3}} \quad (3)$$

For each hydrogel formulation, experiments were performed in triplicates. Averages and their associated standard deviations used as error values are reported.

2.10. Circular dichroism (CD)

To ensure that the mechanical properties of hydrogels fabricated at 40 °C from salmon and bovine GelMA had similar random coil state at the time of photo-crosslinking, and to reveal the cold-adaptation of salmon gelatin and salmon GelMA as a biomaterial with lower capacity of helix formation, circular dichroism was used to confirm conformational changes in secondary structures, aggregation state or triple helix formation. Briefly, solutions of tested materials were made at a 0.1% (w/v) concentration in distilled water. The solutions were then placed on an orbital shaker at 40 °C for 1 h to ensure complete dissolution. Solutions were used immediately for CD analysis. The CD spectra of neat salmon/bovine gelatin and the methacrylamide gelatins thereof were collected using a Chirascan Plus Circular Dichroism Spectrometer (Applied Photophysics Limited, UK). Three spectral scans were performed on each sample at each wavelength of light ranging from 180 to 260 nm with 0.5 nm increments and with a dwell time of 0.5 s, along with a baseline scan of distilled water. Solutions were pipetted into a quartz cuvette cell of path-length 100 μm. Control spectra were generated for each sample after heating and holding at 40 °C isothermally for 120 min. This ensured that equilibrium was reached above the helix

to coil transition temperature. Samples were then placed into a cold room at 4 °C and removed to obtain a repeat spectral scan after 120 min of incubation. Before the scan, samples were again held within the spectrometer at 4 °C for five additional minutes to allow thermal equilibrium below the helix to coil transition temperature. The final data was averaged over the three scans and the baseline subtracted.

2.11. Scanning electron microscopy

A 7% (w/v) gelatin solutions with 0.2% (w/v) PI was prepared as above mentioned, and poured on a Petri dish of 60 mm in diameter for photocrosslinking under UV irradiation (2 min, 261 mW/cm^2 at a wavelength of 365 nm). Photo-crosslinked hydrogels were then cooled at 4 °C for 2 days, frozen at −20 °C for 24 h and kept at −80 °C for 24 h, and finally freeze-dried. This procedure was chosen to control pore structural damage due to ice crystal formation. For microscopic inspection, 1 cm^2 pieces were cut, mounted onto aluminum SEM stubs with double-sided carbon tape and sputter coated with gold-palladium (80/20). Scanning electron microscopy (SEM) (Jeol JSM-25-SII, Japan) was used for microstructure imaging. Scaffold pore size was evaluated using ImageJ software and the same scale bar available on the analysis software installed in the microscope platform. To measure the pore diameters, the oval to circular equivalent diameter calculations was conducted as Heyt & Diaz [38]. First, to quantify the cross-section area A of the oval pores in the SEM section, the equation

$$A = \frac{\pi ab}{4} \tag{4}$$

was applied where a is the major length of the oval pore, and b is the minor length of the oval pore. Afterward, the equivalent diameter D is calculated using the equation:

$$D = \sqrt{\frac{4A}{\pi}} \tag{5}$$

Average diameter values were calculated from 100 pores per hydrogel type and their associated standard deviations used as error values are reported.

2.12. Thermodynamic evaluation of enzymatic hydrolysis

To identify enzymatic advantages and the enthalpic dependency of a proteolytic bioreaction of a Clostripain enzyme from Clostridium histolyticum (CLS-2, Worthington, USA) using either BG or SG, k_{cat} and K_m parameters were calculated at different temperatures in order to obtain the activation energy (E_a) and binding energy (ΔG_{Bind}) using the Arrhenius equation. Before the experiment appropriate enzyme and gelatin concentrations, and reaction times for these assays, were determined based on a product versus time progression curve using different concentrations of substrate and enzyme. This procedure defined the experimental setting to ensure acquisition of initial reaction rates, corresponding to the initial and linear slope of the progression curve. According to the previous experimental settings, bovine and salmon gelatin solutions were prepared in PBS 1× (pH 7.4) at a concentration between 0.8 and 0.025% (w/v) and incubated with 59 U/ml of collagenase type 2 (0.21 mg/ml CLS-2, Worthington, USA) for 30 min at different temperatures (5 °C, 17 °C, 27 °C and 35 °C). Reactions were stopped by denaturating the enzyme at 95 °C for 7 min. To quantify the enzymatic reaction, new primary amine formation after hydrolysis was calculated using the OPA method described above. As a control assay (unspecific hydrolysis) the same set of experiments with different gelatin concentrations (but without enzyme) were conducted at the different temperatures. To determine the activation energy (E_a), binding free energy (ΔG_{Bind}) and the energy of catalytic efficiency (ΔG_{Eff}), the equations

$$k_{cat} = Ae^{-E_a/RT} \rightarrow \ln(k_{cat}) = \ln(A) - (E_a/R)\frac{1}{T} \tag{6}$$

$$K_m = Be^{-\Delta G_{Bind}/RT} \rightarrow \ln(K_m) = \ln(B) - (\Delta G_{Bind}/R)\frac{1}{T} \tag{7}$$

$$\frac{k_{cat}}{K_m} = Ce^{-\Delta G_{Eff}/RT} \rightarrow \ln\left(\frac{k_{cat}}{K_m}\right) = \ln(C) - (\Delta G_{Eff}/R)\frac{1}{T} \tag{8}$$

were used. R corresponds to the ideal gas constant and T to the temperature in Kelvin, whereas A, B and C are constants in the equation. Experiments were performed in triplicates for each condition (substrate concentration v/s temperature).

2.13. Hydrolysis of hydrogels with collagenase type 2

In order to evaluate the capacity of protease-based remodeling of the GelMA hydrogels *in vitro*, different hydrogels, including the two types of gelatin sources and different degrees of functionalization, were subjected to enzymatic hydrolysis using a collagenase type 2 (#CLS-2, Worthington, USA). Biocatalytic reaction conditions were as followed: cylindrical 10% gelatin hydrogels were fabricated as described previously (ø 10 mm, h = 3.14 mm, GelMA 10% (w/v), PI 0.2% (w/v), 261 mW/cm2, for 2 min). Hydrogels were submitted to collagenase hydrolysis in 2 ml of PBS 1× supplemented with 1 U/ml or 50 U/ml of collagenase for 4 h to 20 h at 37 °C. According to the provider, one-unit (U) releases 1 μmol of L-leucine equivalents from collagen in 5 h at 37 °C, pH 7.5. Incubation was performed using an orbital shaker agitation (80 rpm) in well plates. Supernatant samples were obtained after different time intervals and stored at −20 °C for subsequent hydrolysis evaluation and quantification. Quantification of hydrogel hydrolysis was carried out through the identification of new primary amine detection in the supernatant generated after peptide bond cleavage, using the OPA assay, described above.

2.14. Cell culture and fabrication of cell-laden hydrogels

HUV-EC-C [HUVEC] (ATCC® CRL1730™) cells and bone marrow mesenchymal stem cells (BM-MSCs) (#PT-2501, LONZA, Switzerland) were cultured in high glucose Dulbecco's Modified Eagle Medium (DMEM) (#10313, Gibco, USA) supplemented with 2 mM glutamine (#25030-081, Gibco, USA), 10% fetal bovine serum (#16000-044, Gibco, USA) and 1% penicillin-streptomycin (#15140-122, Gibco, USA) using standard T-flasks. Cultures were maintained in an incubator at 37 °C and 96% humidity with a 5% CO_2 enriched air atmosphere. Media changes were performed every 2–3 days and cells passaged using trypsin when 80% cell confluence was reached. HUVEC cells where primarily used for viability and proliferation, since they were previously identified as oxidative-stress sensible cells [39,40], and therefore more sensitive to free radical polymerization. BM-MSCs were used for cell invasion evaluation due to their known migratory activity across hydrogels [41]. For HUVEC cell-laden hydrogels fabrication, GelMA 10% (w/v) and PI 0.2% (w/v) solutions reconstituted in PBS 1× (pH 7.4) were mixed with cells previously washed in PBS 1× (pH 7.4) at 37 °C, to reach typical final concentration of 1 × 10^6 cells/ml. Photocrosslinking of the mixture mounted in a PDMS cylindrical mold was conducted as previously described.

2.15. Cell proliferation assay

In order to evaluate cytotoxicity and comparative cell proliferation compatibility, cell proliferation assessment of encapsulated HUVECs in the crosslinked hydrogels was performed using the WST-1 Cell Proliferation Colorimetric Assay Kit (#K302, Biovision, USA) following the manufacturer's instructions. Briefly, 30 μl of the pre-crosslinked mixture (GelMA 10% (w/v), PI 0.2% (w/v) and 1 × 10^6 cells/ml in PBS 1×, pH 7.4) was poured in a 96-wells plate and crosslinked as stated

earlier. Encapsulated cells were then cultured for 11 days and proliferation was quantified at days 1, 4 and 11. For proliferation assessment, WST-1 was mixed with fresh media (1:9 ratio) and added to the encapsulated cells. After 120 min of incubation at 37 °C in a cell incubator, supernatant absorbance was quantified at 450 nm (Infinite 200 PRO, TECAN, Switzerland). Proliferation is then observed by the increment in absorbance signal at the different day intervals.

2.16. In vitro cell invasion assay

Cell invasion is typically understood as cell migration activity across a 3D extracellular matrix. Cells typically migrate through their environment by remodelling the sorrounding matrix via the use of extracellular metalloproteinases, which play a key role in the process. Using a Boyden chamber system (Transwell®, Corning, USA) for 24 multiwell culture plates, 70 μl of pre-crosslinked GelMA base formulation was carefully added onto the surface of a gelatin-treated porous membrane in a Transwell device (8 μm pore size). Afterwards, hydrogels were photo-crosslinked as described previously and 3×10^4 human BM-MCSs cells were seeded on top of the GelMA based-hydrogels. Incubation was performed with 100 μl of high glucose Dulbecco's Modified Eagle Medium (DMEM) supplemented with 2 mM glutamine and 1% penicillin-streptomycin in the upper chamber and 600 μl of DMEM supplemented with 2 mM glutamine, 10% fetal bovine serum (#16000-044, Gibco, USA) and 1% penicillin-streptomycin in the bottom chamber. Cultures were maintained in an incubator at 37 °C and 96% humidity with a 5% CO_2 enriched air atmosphere for 20 h before analysis. To quantify cell invasion, non-migrating cells in the upper side of the porous membrane were carefully removed by scrapping the hydrogel and cells with a cotton swap. Migrated cells at the bottom side of the membrane were visualized and counted using Crystal Violette staining [42] and inversed microscopy (BX53, Olympus, Japan). As an internal assay control, cell invasion experiments were performed using Matrigel hydrogels (#356234, BD Biosciences) at a 1:4 dilution in PBS. The specific dilution was carefully adjusted to obtain a 35% percent of the maximum possible migration result, therefore, increased or decreased values of migration could be easily distinguished. After pouring 70 μl of Matrigel on the porous membrane, 30 min of incubation at 37 °C prior to the assay was performed to generate the Matrigel hydrogel, following supplier's instructions.

2.17. In vivo hydrogel degradation

To evaluate comparative *in vivo* hydrogel degradation, cylindrical hydrogels of 10 mm in diameter and 3.14 mm in height were fabricated using the GelMA base formulation as previously described. Hydrogels based on salmon and bovine GelMA with low and high degree of functionalization (S0.5M, S5M, B0.5M, B5M) were fabricated and implanted subcutaneously in a mice model. For this purpose, six- to eight-week-old C57BL/6 wild-type mice from the Jackson Laboratory (USA) were used in this study. Experiments were carried out at the Universidad de los Andes-Cells for Cells Animal Facility (Santiago, Chile) following the institutional guidelines for care and experimentation with laboratory animals, and approval from the Institutional Ethical Committee at Universidad de los Andes. Subcutaneous implantations of hydrogels were conducted through a dorsal incision, implantation of individual hydrogels and suturing on anesthetized mice maintained under vaporized sevoflurane (Baxter, USA). Allogeneic skin grafting (skin donor: F1 mice, of BALB/c × C57Bl/6 breeding) was included as a control of transplant rejection and performed as described previously [43]. Briefly, tail skin (~1 cm^2) from F1 mice (BALB/c × C57Bl/6) donors was transplanted onto the dorsal area of C57BL/6 mice. Transplant survival was monitored 3 times per week. At day 14-post surgery the hydrogels were recovered and photographed, then half processed for histological analysis (as explained above), and the other half was cultured for 24 h for cell lineage determination using flow cytometry. Three mice per hydrogel type were used for this experiment.

2.18. In vivo tissue integration and angiogenesis

Cell-laden hydrogels based on modified bovine and salmon gelatin at 60%, 80% and 90% functionalization were fabricated and subcutaneously implanted in 8 weeks NSG™, NOD scid gamma mice (The Jackson Laboratory, USA). Experiments were carried out at the Universidad de los Andes-Cells for Cells Animal Facility (Santiago, Chile) following the institutional guidelines for care and experimentation with laboratory animals, and the approval from the Institutional Ethical Committee. Previous experimental settings were explored in order to formulate cell-laden hydrogels capable to induce hydrogel vascularization *in vivo* within 3 weeks. A mixture of 5×10^5 HUVEC cells and 5×10^5 MSCs were encapsulated in gelatin hydrogels of 8 mm in diameter, 4 mm height (200 μl) and supplemented with 50 ng/ml of recombinant human VEGF 165 (#293-VE, R&D Systems, USA). For photo-crosslinking, UV irradiation (365 nm wavelength) of 46.7 mW/cm^2 for 3 min was applied. Subcutaneous implantation of hydrogels was performed through a dorsal incision then suturing in anesthetized mice under vaporized sevoflurane (Baxter, USA). After 3 weeks, during which mice received food and water *ad libitum*, images of the explanted hydrogels were obtained using a stereomicroscope (SZ51, Olympus, Japan) and the samples prepared for histological analysis. Briefly, hydrogels were fixed in 10% formalin solution (HT501128, Sigma, USA), dehydrated and embedded in paraffin following standard methods. Sections of 5-μm were stained with hematoxylin and eosin (H&E), and Van Gieson's method performed in accordance with standard protocols.

For blood vessel identification, immunohistochemical detection using anti-CD31 reaction was carried out following manufacturer's instructions. Briefly, paraffin sections were pre-treated with xylene and subjected to decreasing concentrations of ethanol. Antigen recovery for CD31 was performed in a pressurized cooker for 3 min (sodium citrate buffer, pH 6). Tissue hydrogen peroxidase activity was avoided after incubation of sections with 3% H_2O_2 for 15 min. Subsequently, sections were incubated with 10% horse serum solution for 30 min for immunoblocking. Sections were later incubated with anti-CD31 antibody (ab28364, Abcam) for 30 min at 25 °C. Antibody detection was resolved using the Envision system (K5007; Dako) with 3–30 diaminobenzidine (SK 4001; Vector, Burlingame, CA, USA) according to the manufacturer's instruction.

Density of formed vessels (vessels/mm^2) within the implanted hydrogels was calculated as the average number of vessels identify by the presence of erythrocyte in the luminal part and the detection through anti-CD31 immunostaining. This analysis was performed using paraffin embedded hydrogel sections from a transversal cut of the hydrogel disc at the mid-point distant, between the bottom and top face of the implants; the entire area of each section was analyzed. Values reported for each experimental condition correspond to the mean ± S.E. obtained from six individual explanted hydrogels. Vessel lumen sizes of each vessel was measured using ImageJ software. Sections were stained with H&E and Van Gieson's method, and cell repopulation reported as the average number of cell-covered area in the hydrogel slides. A tissue integration score was proposed for this study, including a value for the scaffold cell invasion or repopulation (CI), number of vessels (VN) and the vessel luminal area (LA). A weighted score model was applied, considering CI with a 50% weight, VN with a 25% weight and LA with another 25% weight. Therefore, the calculated “tissue integration index” (TI) is obtained from the following equation: $TI = (CI \times 0.5) + (VN \times 0.25) + (LA \times 0.25)$, and normalized (1-100). In the model, the level of vascularization is considered based on parameters VN and LA, while the amount of cell within the scaffolds by CI.

3. Results

3.1. Characterization of commercial bovine gelatin and extracted salmon gelatin

Information derived from SDS-PAGE, amino acid composition analysis and OPA assay were used to estimate comparatively the hydrolysis level between the two types of extracted gelatin. Visual inspection of the SDS-PAGE (Fig. S1a) indicates that SG α_1, α_2 and β subunits have a lower molecular weight compared with BG subunits (110, 130 and 250 kDa *versus* 130, 150 and 270 kDa respectively). The distribution of smaller hydrolyzed polypeptides is, however, similar for both gelatins. On the other hand, the amino acid composition analysis (Table S1, supporting information) of SG and BG gelatin showed a higher amount of lysine in BG (9% higher amount of lysine per 100 g of sample). As for the OPA assay, the indistinctive quantification of α-amino groups from the NH_2-terminal of polypeptides and ε-amino groups of lysines, demonstrated 9% more primary amino groups available for methacrylamide functionalization. Considering the slight reduction in the number of lysine in the case of SG, it is inferred that SG and BG have a similar degree of hydrolysis, otherwise the OPA results would have resulted in a broader relative difference in quantification due to exposed α-amino groups from the NH_2-terminal amine after hydrolysis, not observed in our study (see Fig. S1b). The observed differences between the two types of gelatins *in vitro* and *in vivo* (described in full further below), could be explained by the different nature of salmon and bovine gelatin and not due to differences in molecular weight, hydrolysis degree or number of reactive amino groups per monomer of polypeptides. Although the analysis of gelatin hydrolysis subjected during the functionalization reaction is not included in this study, this phenomenon cannot be discarded [44]. As a result, this study assumes that changes in polydispersity due to gelatin hydrolysis during the functionalization reaction are equivalent between the two type of gelatin for the same condition of functionalization.

3.2. Characterization of bovine and salmon methacrylamide gelatin

During gelatin functionalization, methacrylic anhydride reacts preferentially with primary amine groups of lysine resulting in a gelatin with methacrylamide groups or GelMA [33]. By changing the concentration of methacrylic anhydride, different degrees of functionalization at lysine should be obtained, and therefore hydrogels with different levels of inter- and intra-polymeric crosslinking could be fabricated. In this work, the degree of functionalization was determined by the OPA assay [32] and by ^{1}H NMR spectra analysis and expressed as the percentage of substituted primary amine groups (α-amino groups from the NH_2-terminal and ε-amino groups of lysine in the polypeptide). Samples of salmon and bovine gelatin with different degrees of functionalization were prepared mixing gelatin with methacrylic anhydride (MAA) at 0.5, 2, 5 and 10% (v/v) as described in materials and methods. From here on, salmon samples obtained from those reactions will be referred to as S0.5M, S2M, S5M and S10M respectively and bovine samples as B0.5M, B2M, B5M and B10M respectively.

The obtained values in the OPA assay are presented in Table 1. Results for SG and BG were considered as 0% functionalization at primary amines. The more MAA was added to the reaction, the degree of functionalization increased, reaching approximately 90% substitution at lysine amino acids in S10M and B10M samples.

The analysis of the obtained ^{1}H NMR spectra for all studied samples (spectra shown in Fig. S2) was performed as previously described [34]. The decrease in the peak II at d = 2.9 ppm is associated with a reduction of lysine methylene, which demonstrates the methacrylamine functionalization of lysine. Quantification of lysine methacrylamide substitution obtained with ^{1}H NMR spectra analysis is presented in Table 1. These values are similar to those obtained by OPA assay. Under this premise, the average percentage of substituted lysines is similar for samples treated under the same reaction conditions, regardless of the animal source. These results must be taken carefully since the proposed ^{1}H NMR spectra analysis cannot quantify the methacrylate functionalization at hydroxyl or carboxylic groups (methacryloyl groups) [33] (see Table 1 and Fig. S3). The peak identified as I, located at d = 1.8 ppm, represents the methyl function of the methacrylamide and possible methacryloyl groups if present [45]. On the other hand, peaks at d = 5.4 ppm and d = 5.6 ppm in the spectra of all functionalized gelatins can be attributed to acrylic protons of both groups, methacrylamide and methacryloyl. If quantification of functionalization is performed either through the analysis of peak d = 1.8 ppm or peaks d = 5.4 ppm and d = 5.6 ppm [46], the analysis would not distinguish between methacrylamide and methacryloyl groups, therefore functionalization degree relative to the number of lysine amine groups in the gelatin will be overestimated. After functionalization of gelatin in the presence of MAA and under continuous pH adjustment (neutral), an additional peak in the spectra has been observed at d = 6.1 ppm [34,45]. This peak in the ^{1}H NMR spectra has been reported as methyl protons of the methacryloyl groups transfered to hydroxyl or carboxyl functions. To avoid the presence of methacryloyl functionalization, pH adjustment during the reaction was not performed, limiting the functionalization mainly to primary amine groups as observed by Yue et al. [33], which is evidenced by a lack of the peak in the spectra at d = 6.1 ppm in our case. Therefore, similarities between ^{1}H NMR analysis and OPA assay indicate that functionalization occurs mainly in the primary amino groups in the form of methacrylamine substitution, and methacryloyl functionalization could be considered minimal.

Table 1
Characterization of gelatin and GelMA samples. The complete study presented in this work was conducted using the same batch of functionalized gelatins per condition. The methacrylamide degree of functionalization calculated using the ^{1}H NMR spectra was obtained from a unique NMR experiment per sample. NM = not measured.

Sample	Animal source	% (v/v) MAA in the reaction	Average of substituted lysine (%)		Isoelectric point	Zeta potential at pH 7.4 (mV)
			OPA method	^{1}H NMR spectra analysis		
SG	Salmon	–	0	0	~8.5	~1.6
S0.5M	Salmon	0.5	15 ± 4	13	NM	NM
S2M	Salmon	2	62 ± 3	66	~5.5	~−4.8
S5M	Salmon	5	84 ± 4	87	~5.5	~−3.8
S10M	Salmon	10	90 ± 6	93	~5.5	~−1.3
BG	Bovine	–	0	0	~5.5	~−3.1
B0.5M	Bovine	0.5	24 ± 7	22	NM	NM
B2M	Bovine	2	62 ± 2	56	~4.7	~−7.5
B5M	Bovine	5	81 ± 2	79	~4.7	~−7.8
B10M	Bovine	10	87 ± 4	87	~4.7	~−7.8

3.3. Zeta-potential and isoelectric point of the methacrylamide gelatins

Considering the substitution of free amine with methacrylamide groups as a process where only the basic side chains of lysine are involved, a shift in the isoelectric point of the gelatin towards acidic pH is expected (see Table 1 and Fig. S4). This turns gelatin into a more negatively charged polymer at pH 7. The isoelectric point for BG and bovine GelMA solutions are pH ~ 5.5 and ~4.7 respectively, whereas the isoelectric point of SG and salmon GelMA solutions are pH ~ 8.5 and ~5.5 respectively. Importantly at physiological pH 7.4, the zeta-potential, which correlates with the surface charge, was ~ −7.5 mV for all modified bovine gelatins, and as for modified salmon gelatin, the zeta-potential was within the range of ~ −1.3 to ~ −5 mV, depending on the degree of functionalization. Due to the alkali extraction protocol used for bovine gelatin type B, an extended percentage of asparagine

Table 2
Melting characterization of gelatin solutions (7% w/v) in a non-functionalized and functionalized state.

	SG	S10M	BG	B10M
T_m (°C)	4.26 ± 0.03	4.09 ± 0.08	12.20 ± 0.01	9.69 ± 0.20
ΔH_m (J/g)	0.88 ± 0.03	0.48 ± 0.09	1.20 ± 0.02	0.73 ± 0.01
ΔT (°C)	11.19 ± 0.02	10.97 ± 0.14	19.72 ± 0.01	17.46 ± 0.16

Results are shown as average (± standard deviation).

and glutamine deaminate into aspartate and glutamate occurs. This results in a more negatively charged protein compared to salmon gelatin [47]. In addition, the zeta-potential value at neutral pH is slightly more negative for BG as compared to SG, which is also true for comparisons between GelMAs of the two species at equivalent degrees of functionalization (see Table 1).

3.4. Thermophysical properties of the methacrylamide gelatins

The melting temperature (T_m) and enthalpy (ΔH_m) of salmon and bovine gelatin solutions (7% w/v) were evaluated using differential scanning calorimetry (DSC). As reported in Table 2, the T_m of salmon gelatin (4.3 °C) is significantly lower than the T_m of bovine gelatin (12.2 °C). When SG and BG were functionalized (S10M and B10M respectively), the melting temperatures decreased significantly towards a lower temperature in both cases ($p < 0.05$, *t*-test). The T_m of modified salmon gelatin is, as expected, considerably lower than for modified bovine gelatin ($p < 0.05$, *t*-test).

To understand the influence of concentration and degree of functionalization in the different parameters of salmon gelatin melting behavior (T_m, ΔH_m, ΔT), a factorial experiment design (2 levels with center point) was performed as described in the Material and methods section. Fig. S5 shows the magnitude of the effect and it's significance on the different parameters ("effects plots"), and the graphical representation of variable interaction and range of parameters ("contour plots"). At least for salmon gelatin, functionalization degree (64% v/s 94%) did not significantly affect the T_m, which is expected due to the slight differences already observed for SG and the highly functionalized salmon gelatin (S10M) (see Table 2). Concerning ΔH_m, that indirectly quantified the stability and quantity of formed triple helix, only the concentration variable demonstrated a significant influence, whereas a change of functionalization degree from 64% to 94% did not affect ΔH_m, possibly because a further increment in functionalization or disruption of lysine residues does not further destabilize the free energy of triple helix [48]. However, functionalization degree significantly affects the endothermic transition width (ΔT) ($p < 0.05$), which in this case comparatively reflects the dispersity of triple helix length or stability. In the case of highly functionalized gelatin, shortening of ΔT respond to a less disperse distribution of helix formation in terms of length or energetic stability, that could be attributed to a complete and homogeneous substitution of lysine in all polypeptides. These data corroborate the importance of lysine in the stability of triple helix formation as reported in a previous study [49]. Finally, we did not observe a significant effect explained by the interaction between the functionalization degree and gelatin concentration factors over T_m, ΔH_m or ΔT ($p > 0.05$), indicating that these formulations likely do not present synergic phenomena in relation to their melting behavior.

3.5. Mechanical properties of the methacrylamide gelatins

Compressive and Young's moduli of hydrogels fabricated with salmon and bovine GelMA with different degrees of functionalization are presented in Fig. 1a-b. All hydrogels were fabricated at 40 °C to avoid triple helix formation before photo-crosslinking, therefore, all observed differences are associated to the gelatin source and the degree

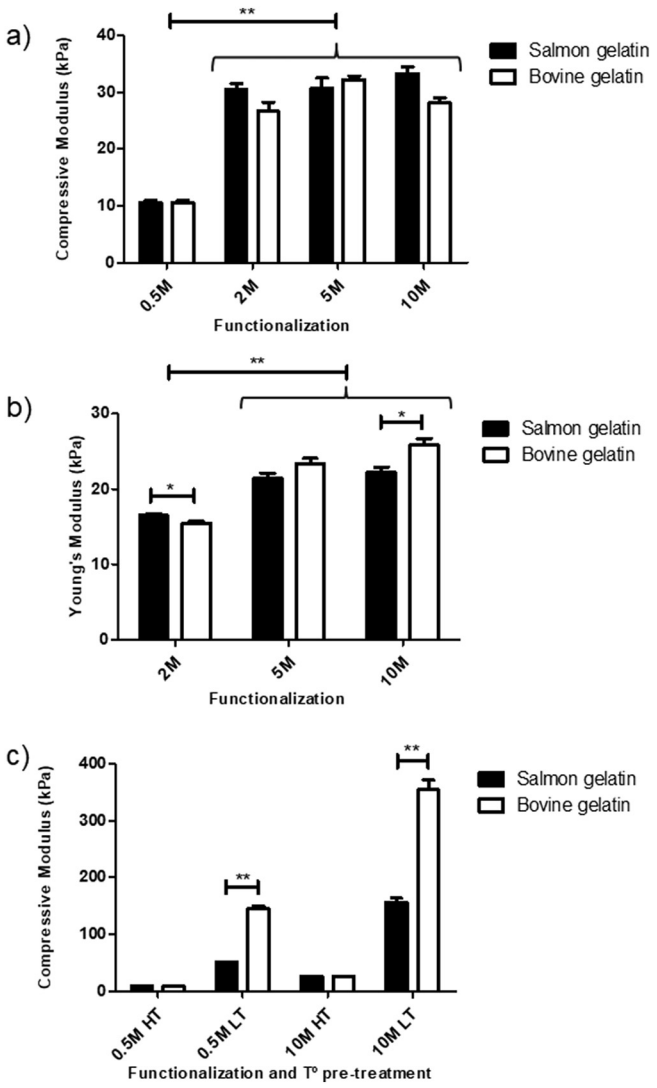

Fig. 1. a) Comparison of the mean compressive modulus values of salmon- and bovine-gelatin-derived hydrogels. b) Comparison of the mean values of Young's modulus obtained from tensile testing. c) Graphical comparison of the mean compressive modulus values of salmon- and bovine-gelatin-derived hydrogels. One set of hydrogels were fabricated and photo-crosslinked at 40 °C (HT), whereas a second set was cold-annealed for 2 h at 4 °C and photo-crosslinked at 4 °C (LT). *$p < 0.05$; **$p < 0.01$ (Mann-Whitney), n = 5–6.

of functionalization, and not to the quantity of triple-helix formation or physical cross-linking before photo-crosslinking. The compressive modulus was found to increase upon increasing degree of functionalization, showing a positive correlation. The compressive modulus of S0.5M and B0.5M hydrogels was significantly increased from 11 kPa (10.6 ± 0.3 kPa and 10.5 ± 0.5 kPa, respectively) to 30.5 ± 1.0 and 26.6 ± 1.6 kPa respectively when functionalization increased to ~60% (S2M and B2M). However, it does not appear to increase further with higher degrees of functionalization in both gelatin types. Overall, neither hydrogels derived from salmon GelMA nor from bovine GelMA has managed to outcompete the other in terms of compressive modulus.

In relation to the Young's modulus measurements (tensile), neither hydrogels using the salmon- nor bovine-derived gelatin at the lowest degree of functionalization (S0.5M and B0.5M respectively) were of sufficient integrity to enable tensile testing. However, the results obtained from hydrogels derived from GelMA with a degree of lysine substitution from ~60% (2 M) to 90% (10 M) showed a positive correlation with the Young's modulus, as previously [17]. In general, the small changes in degree of methacrylamide substitution are reflected in

the mechanical testing with good correlation, and no significant difference in mechanical behavior is observed between photo-crosslinked salmon and bovine GelMA.

To explore the mechanical improvement attained by pre-formation of triple-helices before photo-crosslinking, hydrogels were subjected to 2 h of annealing at 4 °C followed by photo-crosslinking at the same temperature as describe in the Materials and methods section. As shown in Fig. 1c, the thermal stabilization of the structure by prior formed triple helices before photo-crosslinking, delivers a significant increase in compressive modulus. S0.5M hydrogels reached a 6-fold increase as well as S10M, whereas both B0.5M and B10M achieved a 15-fold increase in compressive modulus. These results agree with the differences in the enthalpy of transition (ΔH_m) between the two sources of gelatin describe in the DSC analysis of melting behavior, demonstrating a higher energetic stabilization of triple helices in the case of warm-adapted (mammalian source) gelatin compare to cold-adapted (salmon source) gelatin as described for non-functionalized gelatin in previous studies [24,25].

3.6. Molecular mobility of the methacrylamide of gelatin-based hydrogels

Because it has been argued that mechanical properties and the rate of enzymatic hydrolysis can be influenced by the polypeptide flexibility of gelatin, the mobility of structure of gelatin at the molecular level in photo-crosslinked hydrogels was studied by NMR relaxation time using T_2 measurements. As explained in the material and method section, the signal component from the polymeric fraction and water population was extracted from the echo decay curves. In Fig. 2a, the reciprocal of relaxation times T_{2e1} for the polymer fraction in the sample is presented for hydrogels based on salmon and bovine gelatin at different degrees of functionalization (S2M, S5M and S10M, and B2M, B5M and B10M respectively). In general terms, photo-crosslinked hydrogels based on salmon gelatin showed longer relaxation times (*i.e.* higher chain mobility) than photo-crosslinked bovine gelatin. On the other hand, both biomaterials present a systematic decrease in the observed relaxation time as the degree of functionalization increases. The same effect also holds true for the average relaxation rate of the water phase, calculated as described in the Materials and methods section. Fig. 2b indicates that the water molecules contained in the salmon and bovine gelatin-based hydrogels are substantially restricted in their mobility (reduced T_2 time) upon increase in the amount of substituted lysines. It can be expected that T_2 relaxation times are associated to the total density of mobility constrainers, such as covalent crosslinking and the entanglements of gelatin polypeptides [50]. Hence, the molecular mobility in the bovine gelatin-based hydrogels is significantly lower than in the salmon gelatin-based hydrogels. These data correlate well with the degree of functionalization, measured as the percentage of substituted lysine (R^2 = 0.94 and 0.98 for salmon and bovine gelatin-derived hydrogels respectively). Moreover, changes in relaxation times follow the trend in DSC results in terms of triple content as reflected by the differences in ΔH_m between both gelatin sources (see Table 2).

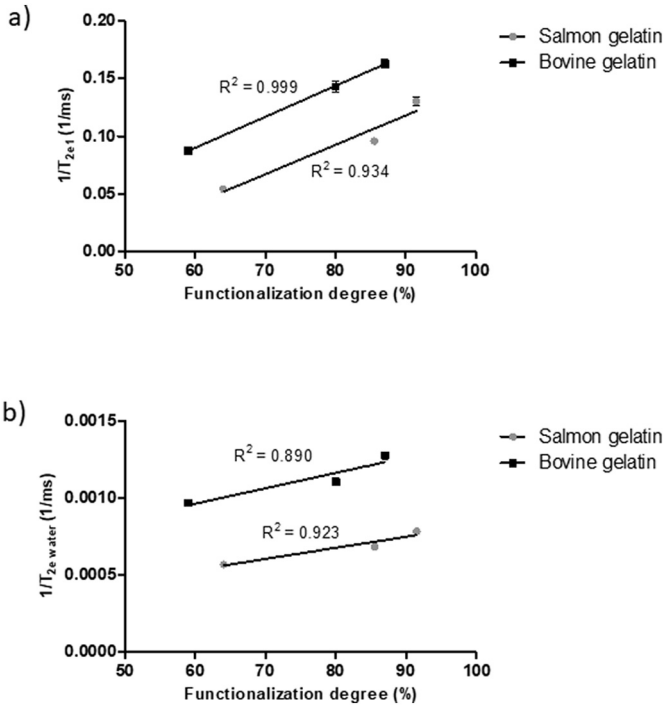

Fig. 2. Proton transverse relaxation rates for photo-crosslinked hydrogels at different degrees of functionalization. a) Gelatin polymer component and b) water component inside the gelatin hydrogel. Error bars are sometimes smaller than the size of the symbols in the plot.

3.7. Circular dichroism of salmon and bovine gelatin and the respective GelMA

Circular dichroism (CD) spectroscopy is a well-established technique capable of determining the secondary structure of proteins in solution [51]. The technique is based on predefined spectroscopic signatures of well-known structures. Of specific interest in this study is that of the collagen triple helix with a distinct positive peak at 220 nm and a negative peak at 200 nm. The relative degree of thermally induced "random coil to triple helix" transformation on cooling can be qualitatively described by comparing between samples the shape of the CD curves and the associated magnitude of their peaks [52]. The cold-adaptated salmon gelatin displayed a lower capacity of thermally induced random coil to triple helix transformation upon cooling (Fig. S6). Additionally, the presence of methacrylamide groups on both source of gelatins reduced the propensity for triple helix formation, especially with respect to the positive peak most associated with the triple helix configuration. It is important to indicate that both bovine and salmon GelMA showed a random coil configuration at 40 °C, therefore hydrogel formation upon UV irradiation at 40 °C was conducted for both sources of gelatin under random coil configuration and that the mechanical properties of hydrogels was not influenced by triple helix (physical) crosslinking before covalent (chemical) photo-crosslinking.

3.8. Microstructure characterization of the mobility of methacrylamide gelatin-based hydrogels

The size of the pores generated in GelMA-based hydrogels after freeze-drying has a negative correlation with the degree of functionalization [53], concentration of photo-initiator in the pre-crosslinked solution [54], and GelMA concentration [55]. Additionally, these parameters of formulation positively correlate with the mechanical properties of formed hydrogel after photo-crosslinking. To understand the effect of the cold-adaptation of salmon gelatin on pore size, comparative studies were conducted for hydrogels derived from salmon and bovine GelMA at different degree of functionalization. Fig. 3 shows SEM images of freeze-dried photo-crosslinked bovine and salmon GelMA hydrogels. For both bovine and salmon GelMA, smaller pore sizes are observed when the degree of methacrylamide functionalization increases, as expected. Interestingly, salmon gelatin-based hydrogels generated larger pore size (see Fig. 3), although hydrogels based on both sources showed similar mechanical properties in Fig. 1 (compressive and Young's modulus). Therefore, differences are prossibly associated with a higher molecular mobility within the salmon gelatin-based hydrogels compared to the bovine counterpart, as shown earlier and further explained in the discussion section.

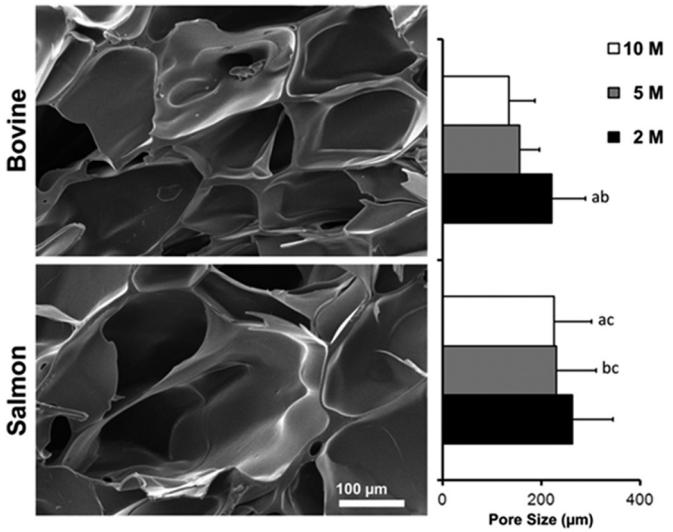

Fig. 3. SEM analysis of photo-crosslinked bovine and salmon GelMA-based hydrogels. Bars with the same letter establish no significant difference between them ($p > 0.05$, Mann-Whitney). (*e.g.* a: bovine 2M = salmon 10M). All other comparisons are significantly different. Three hydrogels per condition were quantified and sizes of all pores were measured using images with 100 µm scale bars. Error bars = S.D.

3.9. Thermodynamic evaluation of enzymatic hydrolysis of SG and BG

Previous reports have associated higher mobility of substrate during enzymatic hydrolysis with improved catalytic efficiency for members of the peptidase family EC3.4, such as metalloproteinases 2, 9 and collagenase type 2 [26,27]. This effect could have important benefits in the yield of cell-active remodeling and vascularization of hydrogels derived from salmon gelatin. An interesting property of salmon gelatin is the lower prevalence of proline and hydroxyproline compared to bovine (see Table SI), rendering salmon gelatin a more flexible polypeptide compared to bovine gelatin [24,25]. This is also reflected in the NMR relaxation experiments (see Fig. 2). This characteristic is typically presented in more flexible protein structures or cold adapted enzymes [56,57], where a lower energy of enthalpy is required for molecular accommodation in the active site of hydrolases and during translocation to a transitional state.

To prove this hypothesis of reduced enthalpic requirements, bovine and salmon gelatin were subjected to enzymatic assays using a general collagenase (CLS-2, Worthington, USA), typically capable of performing ECM remodeling or hydrolysis. According to Arrhenius law, which describes the effect of temperature on the activity of enzymes (see the Materials and methods section) and the relation between the activation energy (Ea) and enzymatic parameters (see materials and methods section), calculation of E_a and ΔG_{Bind} will demonstrate the dependency of temperature for catalytic conversion and substrate binding respectively. To obtain the activation energy (E_a) of the reaction, k_{cat} and K_m parameters were calculated at different temperatures. Lower dependency of SG compared to BG indicates that less need of enthalpic energy is required for salmon gelatin, essentially due to his higher flexibility and therefore, better facilitated translocation to a transitional state during biocatalytic reaction (see Fig. 4).

The activity of collagenase on bovine gelatin showed a lower catalytic constant (k_{cat}) between 5 and 17 °C and higher dissociation constant (K_m) for the all temperatures tested compared to salmon gelatin (see Fig. 4), and as well higher E_a (37.7 kJ mol^{-1} versus 17 kJ mol^{-1}, calculated from 17 to 35 °C), which agree thermodynamically with a higher molecular mobility in the case of salmon gelatin. Interestingly, from 17 °C to 5 °C, there is an important shift in the E_a and ΔG_{Bind} values for both bovine and salmon gelatin, which is more pronounced for

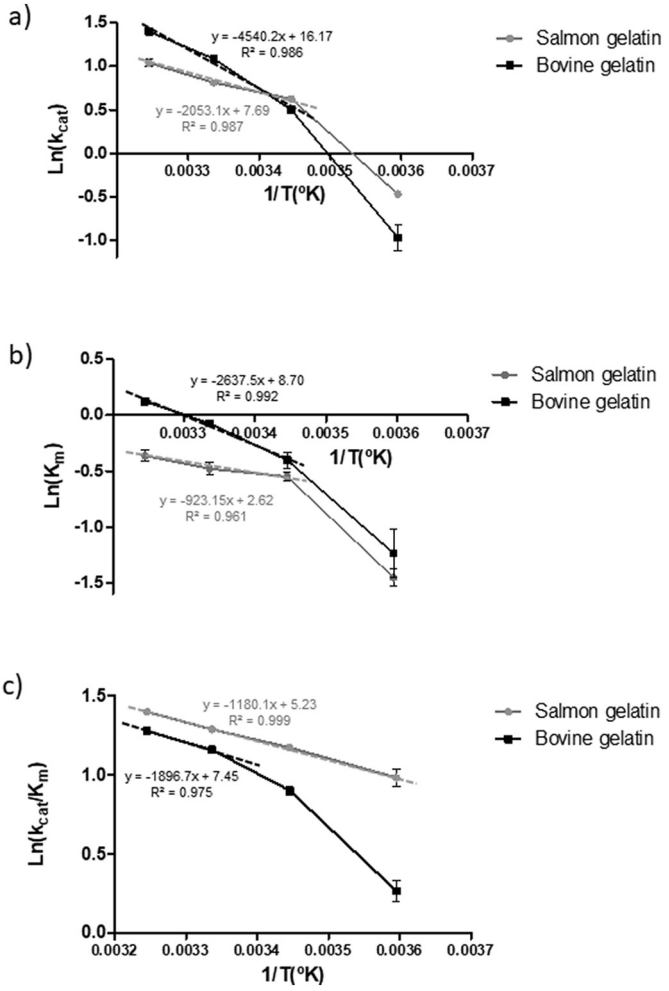

Fig. 4. Activation energy (E_a), binding free energy (ΔG_{Bind}) and energy of catalytic efficiency ($\Delta G_{Efficiency}$) calculated for collagenase type 2 using salmon and bovine gelatin as substrate. K_{cat} and K_m parameters at different temperature were calculated from the result of 3 parallel reactions at different concentrations of bovine and salmon gelatin. E_a, ΔG_{Bind}, and $\Delta G_{Efficiency}$ were calculated using the dashed line slope according to equations in the materials and methods section. Temperature is expressed in °K units which correspond to 35, 26.6, 17.1 and 5 °C respectively. Error bars = S.D.

bovine gelatin and starting to be noticed already at 17 °C. This drifting is reflected in the change in the number and stabilization of triple helices of gelatin during gelation at lower temperature, restricting substrate harboring and reaching of the transitional state at the active site of collagenases. This correlates with the melting behavior of both gelatins in solutions, in which T_m for salmon gelatin is around 4.3 °C while for bovine gelatin 12.2 °C (see Table 2).

3.10. Evaluation of hydrolysis kinetic of the GelMA-based hydrogels

As seen previously, the degree of methacrylamide functionalization could enhance the mechanical properties of photo-crosslinked hydrogels (see Fig. 1), hence tissue engineering applications in which scaffolds are submitted to mechanical challenges, could be favored. However, inclusion of bulky groups along the sequence at lysine amino acids with the concomitant interruption of side chain sequence and higher degree of covalently interconnected hydrogel, could affect the biomaterial harboring and hydrolysis at the catalytic side of ECM-remodeling enzymes, therefore substrate specificity and catalytic efficiency could be compromised. To assess this aspect of biomaterial functionalization, photo-crosslinked hydrogels derived from the two different sources and

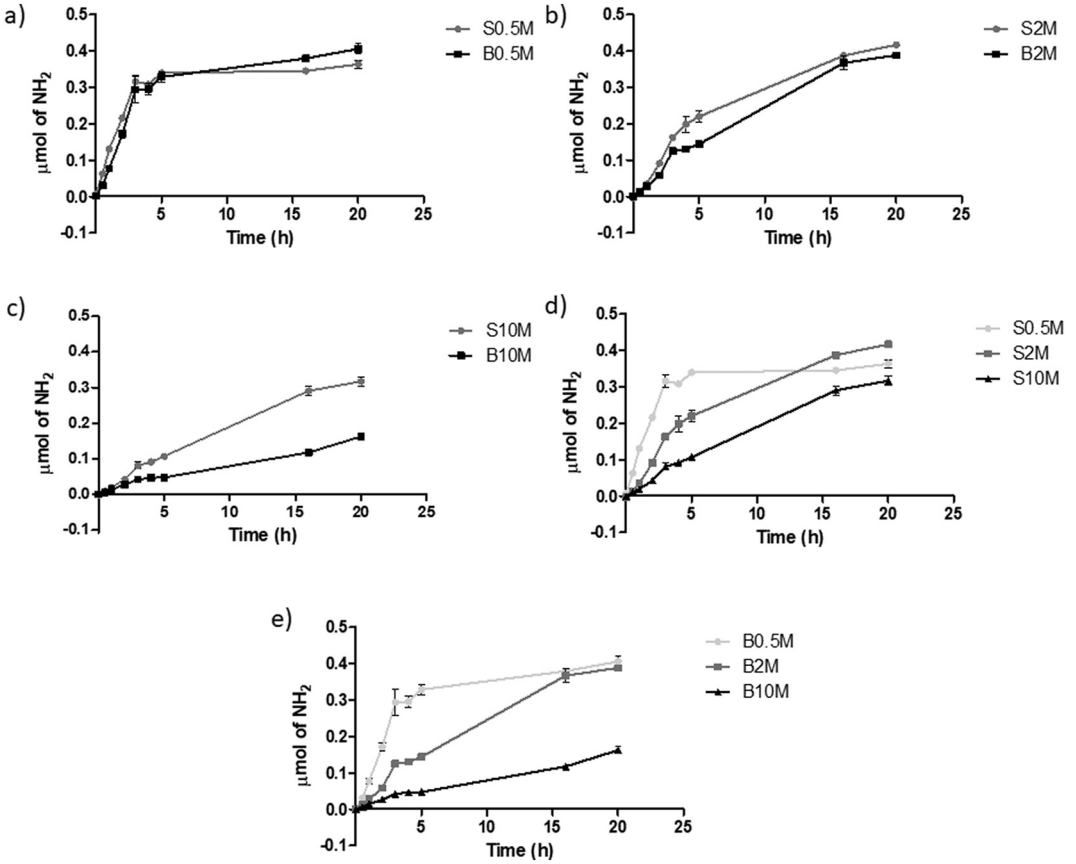

Fig. 5. Progress curves of the hydrolysis of hydrogels by collagenase type 2. Comparative kinetics of hydrolysis between hydrogels derived from gelatin of different sources and similar degrees of functionalization (a)–(c). Comparative kinetics of hydrolysis between hydrogels derived from the same gelatin source but different degrees of functionalization (d)–(e). Hydrolysis reactions at 1 U/ml of enzyme concentration were performed in triplicates at 37 °C and evaluated at different intervals over 20 h. Hydrolysis reaction was performed in triplicates. Error bars = S.D.

different degrees of methacrylamide functionalization were subjected to hydrolysis with collagenase type 2. The kinetics of hydrogel hydrolysis (Fig. 5), exhibit no remarkable differences using either 1 U/ml (see Fig. 5) or 50 U/ml of collagenase (Fig. S7) when comparing salmon and bovine GelMA with similar degree of functionalization, except for hydrogels based on S10M and B10M. At higher degree of functionalization, rate of hydrolysis was faster for salmon GelMA compare to bovine GelMA. In relation to degree of methacrylation, there is a decrease in the rate of hydrolysis when methacrylamide substitution increases.

This similitude in hydrogel hydrolysis turnover is in accordance with the obtained catalytic parameters of collagenase at 37 °C (see Fig. 4). Although the catalytic efficiency (k_{cat}/K_m) of collagenase using salmon gelatin is higher at temperatures below 25 °C, at 37 °C the efficiency is only slightly higher for salmon gelatin.

3.11. Proliferation of encapsulated cells in gelatin hydrogels

To elucidate the effect of greater molecular flexibility of salmon gelatin and the different degree of functionalization on cytocompatibility, cell proliferation assays were conducted using HUVECs embedded within hydrogels and maintained under cell culture conditions. Proliferation was quantified through measurements of mitochondrial metabolic activity at different days' post-encapsulation, showing a slight increment for salmon in comparison to bovine gelatin on day 1 and 5M functionalization degree (see Fig. S8). In general terms, no remarkable differences are observed between salmon and bovine gelatin, and no differences are evident for different degree of methacrylamide functionalization. Similar observations have been reported previously with methacrylamide porcine and cold-fish gelatins [22].

3.12. In vitro cell invasion assay

Although previous results have demonstrated an improved rate of remodeling for salmon GelMA-derived photo-crosslinked hydrogels, it is important to evaluate the activity of cell-derived remodeling triggered by the cells-ECM interaction. Utilizing the classical Boyden chamber (Transwell, Corning, USA) coated with a layer of hydrogel based on the different GelMA and degree of functionalization, capability of the remodeling of hydrogels by mesenchymal stem cells can be tested. As shown in Fig. 6, a higher degree of functionalization limited the capacity of invasion through the biomaterial. Possibly, methacrylamide groups undergoing radical polymerization generate higher compaction and a more intricate gelatin polypeptide network. Restricted molecular mobility of polypeptides, as shown in the NMR relaxation data, in addition with the occupation of lysine side chains by bulky methacrylamide groups, could explain a restriction in efficiency of binding and catalytic activity of metalloproteinases secreted by the cells. This would constrain the advance of cells through the coating material and the porous membrane, hence, a more functionalized material could constitute a biomaterial with less capacity for cell invasion, remodeling and neo-vascular ingrowth.

To understand the extent to which bovine or salmon gelatin of different degrees of functionalization can restrict the invasion and transmigration of cells, a coating of modified gelatin at different concentration (3.0–4.5% w/v) was applied to the porous membranes of Transwell inserts before transmigration assays. Interestingly, bovine gelatin with a degree of methacrylamide functionalization of 60% (S2M) at a concentration of 4.5% (w/v) was still capable of allowing cell migration equivalent to 23% of cell confluency at the bottom face

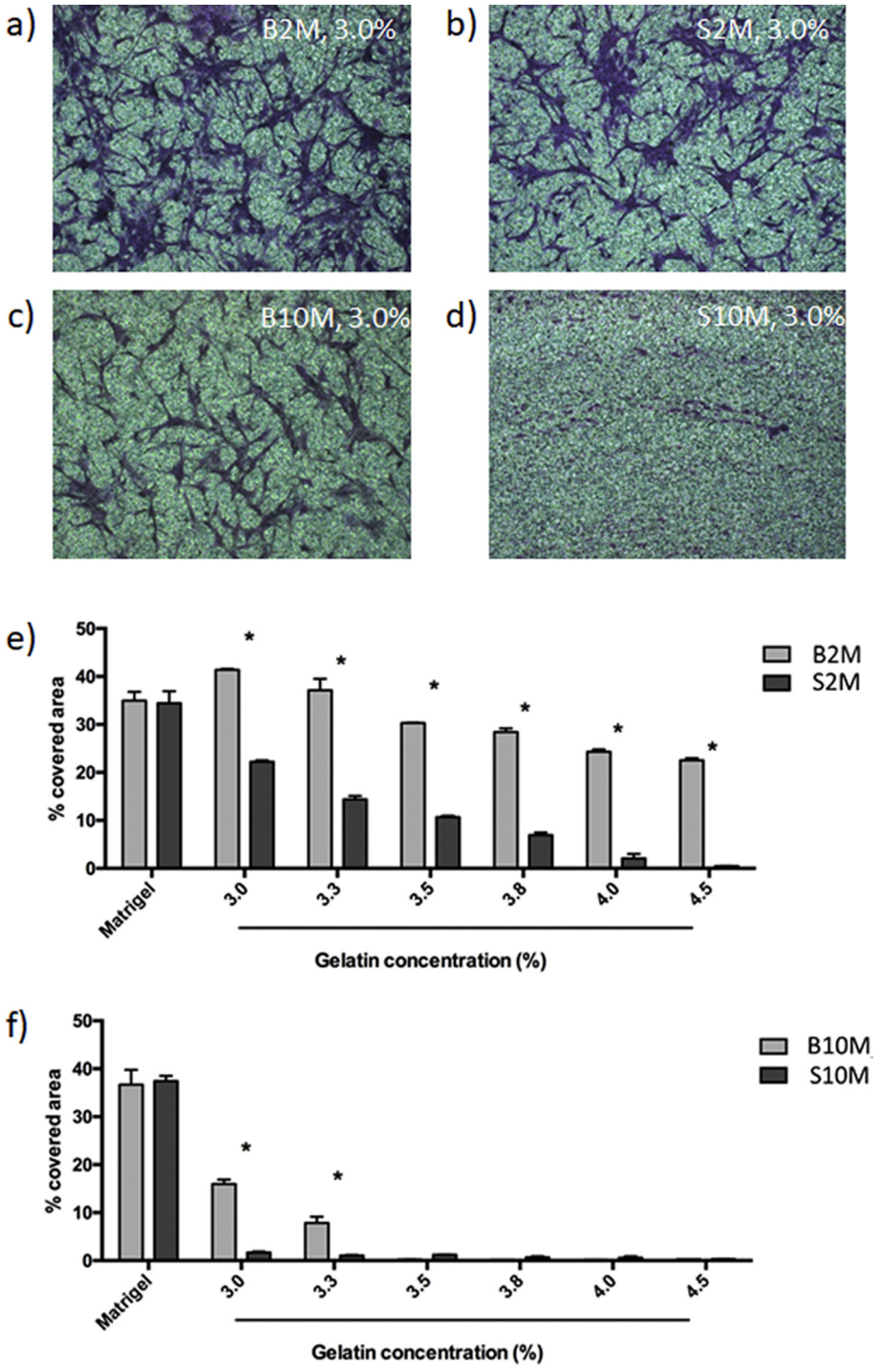

Fig. 6. Capability of hydrogel remodeling using evaluation of BM-MSCs migration across the hydrogel in a Boyden chamber. a) Migration through a 3.0% hydrogel of B2M; b) migration through a 3.0% hydrogel of S2M; c) migration through a 3.0% hydrogel of B10M; d) migration through a 3.0% hydrogel of S10 M. e) Summary graph of cell migration results using B2M and S2M hydrogel barriers at different concentrations. f) Summary graph of cell migration results using B10M and S10M hydrogel barriers at different concentrations. Migration barriers based on matrigel diluted at 1:4 in PBS were used as internal assay control. Error bars = S.D. $*p < 0.05$ in a *t*-test. Experiments were performed in triplicates.

of the porous membrane, while salmon gelatin at 64% of functionalization did not show any migration at 4.5% (w/v) of concentration. On the other hand, 91.5% of lysine functionalization did not show any cell migration for any tested concentrations when salmon GelMA was applied as the hydrogel coating, whereas for bovine GelMA at 87% degree of functionalization and a concentration of 3.3% (w/v) appeared as the upper concentration limit for allowing cell migration in this assay.

3.13. *In vivo* hydrogel degradation

Hydrogels or scaffolds in tissue engineering are usually subjected to remodeling once implanted *in vivo*, which is conducted by the activity of multiple cell types (mesenchymal stem cells (MSCs), endothelial cells, immune cells, fibroblast, among others). Therefore, it is important to prove conceptually the degradation performance in an *in vivo* model. For this purpose, subcutaneous implantation of hydrogels fabricated from salmon and bovine GelMA at 0.5 M and 5 M of functionalization was performed in mice, monitoring them until day 14 post surgery. No signs of inflammation were detected in any of the experimental groups, except for the allogeneic skin graft model, included as an immune rejection control (see material and methods section), this showed rejection around day 9 post surgery, as previously described [43]. As depicted in the Fig. S9, implants were not rejected, and all showed signs of vascularization, advising that cell infiltration and/or migration took place. Hydrogels based on salmon GelMA (S0.5M) were not recovered due to complete degradation. This observation is complemented with

histological analysis (H&E staining), in which infiltration and re-modeling of the matrix occurred with less impairment in hydrogels with lower % of functionalization. Whereas those with ~80% of methacrylamide functionalization (B5M, S5M) showed cells only in the surrounding border of the implants (see Fig. S9). Although the images depict almost no infiltrating cells in B5M- and S5M-based hydrogels, when implants were cut and cultured in media for 24 h, total cells were recovered and identified by flow cytometry as non-hematopoietic ($CD45^-$) and hematopoietic lineage ($CD45^+$) cells. This latter population corresponded to leukocytes including Antigen presenting cells (Dendritic cells, Macrophages and B cells) and T lymphocytes (see Fig. S9), whereas $CD45^-$ cells could be identified as MSCs, endothelial cells and fibroblasts, among others.

3.14. In vivo tissue integration and angiogenesis

To test the capability of tissue integration, and to understand if either the species-dependent gelatin or the different degree of methacrylamide functionalization present barriers for the *in vivo* integration of scaffolds, subcutaneous hydrogel implantations were performed in immunosuppressed mice (NSG mice) and the level of cell re-population and vascularization evaluated. In order to find conditions in which the implanted hydrogels were tissue integrated and vascularized, different combinations of cells and factors were tested and selected. Initially, hydrogels were implanted alone without showing cells repopulation or presence of internal vasculature. Afterward, encapsulation of 50 ng/ml of VEGF were included in the implanted hydrogel without showing the invasion of cells or internal vascularization. Slight improvement could be observed with hydrogels supplemented with 50 ng/ml of VEGF and 1×10^6 encapsulated HUVECs. After replacing HUVECs for mesenchymal stem cells from bone marrow (BM-MSCs), no further improvement was observed again in comparison to HUVECs encapsulation. Surprisingly, a final tested combination of 50 ng/ml of encapsulated VEGF, 5×10^5 HUVECs and 5×10^5 MSCs resulted in a broad cell re-population and profound vascularization of the scaffold (see Fig. S10). BM-MSCs are capable of assisting and stabilizing the formation of blood vessel, hence cell invasion and re-population was improved. A similar phenomenon was reported previously by Khademhosseini and collaborators [53] for porcine GelMA-based hydrogels. Using this combination of factors (VEGF) and cells, all gelatin hydrogels from different sources and degrees of functionalization were tested subcutaneously in NSG mice. As expected, higher levels of cell re-population and vascularization were observed in hydrogels derived from less functionalized gelatins. To perform a comparison of tissue integration among the different experimental groups, a weighted score model was applied, considering cell-repopulation with a 50% weight, whereas number of vascularizing vessels and vessel lumen area were weighted with 25% each. Comparing this score obtained from implanted hydrogels derived from salmon and bovine GelMA at higher degree of functionalization (~90%), improved values for salmon GelMA are observed, whereas with gelatin functionalized at ~62% of lysine, bovine gelatin showed a significantly higher level of cell re-population and vascularization compared to hydrogels derived from salmon gelatin at the same degree of functionalization. Interestingly, besides a higher density of blood vessels, there is a negative correlation between the size of lumen and the degree of functionalization (see Figs. 7 and 8).

4. Discussion

In this work, comparative research has been undertaken using equivalent gelatin preparations in regard to level of hydrolysis and degree of methacrylamide functionalization. The differences observed are mainly attributed to the nature of the amino acid sequence of the source of gelatin. This was demonstrated experimentally by molecular weight analysis by SDS-PAGE, amino acid composition analysis, quantification of free amine using the OPA assay and degree of methacrylamide substitution measured from ^{1}H NMR spectra of gelatin solutions (Fig. 1 and Table 1). In order to comparatively assess SG as a new, cold-adapted biomaterial for tissue engineering, a mammalian functionalized gelatin candidate, namely bovine gelatin type B (BG), was chosen to benchmark against. In this particular case, the methacrylamide functionalized version of BG is considered mechanically tougher and less immunogenic than porcine gelatin (PG), therefore, its advantage in tissue engineering has been established in previous studies [58].

Concerning the electrostatic behavior of gelatin monomers at different pHs, non-modified BG showed a lower isoelectric point (pH 5.5) than SG (pH 8.5); however, when functionalized, the isoelectric point shifted as to become similar among different preparations of functionalized gelatin derived either from bovine (pH 4.7) or salmon (pH 5.5) (see Table 1 and Fig. S3). Differences in isoelectric point and zeta-potential between BG and SG are associated mainly to a higher abundance of negatively charge amino acids (glutamate and aspartate) in BG compared to SG, whereas differences in charge at neutral pH among functionalized gelatins, could be explained by a reduction in the content of primary amine groups as the degree of lysine functionalization increases. All the same, solutions of non-modified and modified gelatins are recommended to be tested for pH and adjusted to pH 7.4 before mixing with or applying cells in order to avoid cytotoxicity, especially for BG. pH adjustment was performed for all experiments in this study, either for salmon and bovine GelMA.

For biofabrication purposes, use of biomaterials in conjunction with diverse technologies of high precision such as 3D bioprinting or microfluidics is highly desirable. The melting behavior of the biomaterials describe the stability of the aggregation states at different temperature, and can therefore determine the capability of biomaterials to be used at certain range of temperature without blocking the dispensing nozzel or channel system due to for example gelation. The lower T_m observed for SG in comparison with BG (see Table 2 and Fig. 2) can be seen as a technological advantage, allowing biofabrication technologies that require stable liquid aggregation states, especially close to room temperature, and to perform appropriately within a broader range of temperatures (broader processing window). On the other hand, the factorial experiment design had as an objective the understanding of polymer interaction during gelation and how methacrylamide groups affect this process from the perspective of total energy of formed triple helices (ΔH_m), or whether the degree of functionalization could affect the size distribution of triple helices (ΔT). In this regard, methacrylation affects the energy of formed triple helices (see Table 2), which is evidenced too in the CD experiments (see Fig. S6). However, it was not significant for changes in the degree of functionalization from 64% to 94% (Fig. S5), which correlates well with the similar mechanical properties shown in Fig. 1. Nonetheless, variability in levels of functionalization resulted in significant differences in (ΔT), possibly due to changes in the size distribution of formed triple helices caused by distinct degree of methacrylamide and the organization of groups in gelatin polypeptides.

Concerning the mechanical properties, changes in degree of methacrylamide substitution are reflected in the mechanical testing with good correlation as previously reported (Fig. 1) [59]. Surprisingly, no differences in mechanical behavior were observed between photo-crosslinked modified gelatin from salmon or bovine, which in one sense aligned with the idea that the degree of hydrolysis, molecular weight and number of methacrylamide groups per monomer is equivalent between both sources of gelatin. However, a previous report [22] demonstrated that hydrogels fabricated with methacrylamide gelatin derived from undefined sources of cold-fish have lower mechanical strength than their porcine counterparts, establishing that the possible reasons are related to the different amino acid composition and to a certain extent, to the molecular weight distribution. Interestingly, and in accordance with our results, it could be debated that under the photo-crosslinking condition used in this study (40 °C, random coil

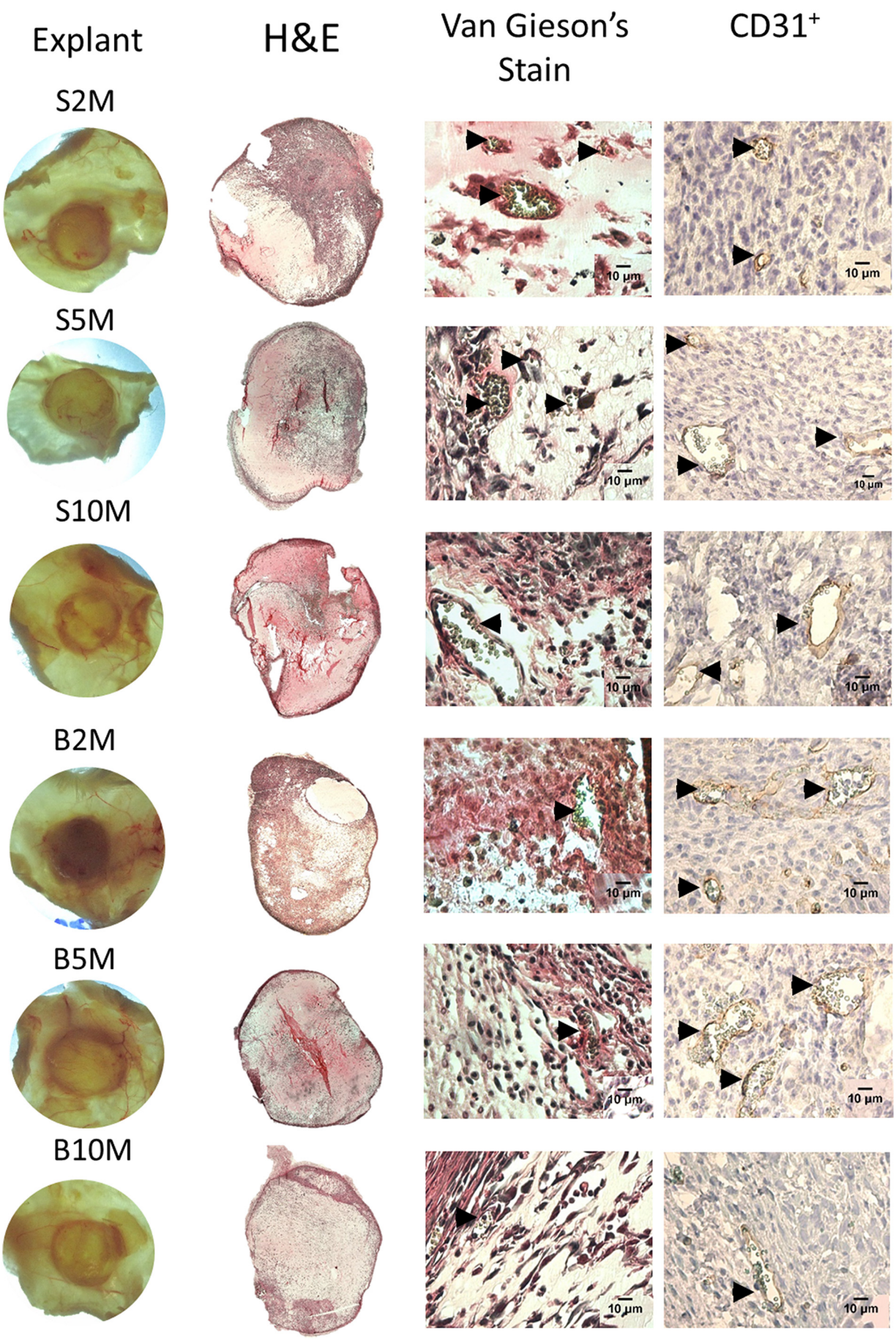

(caption on next page)

Fig. 7. Hydrogels cell repopulation and vascularization *in vivo*. Comparative examples of explanted hydrogels derived from gelatin from different sources and degrees of functionalization are shown. Consecutive images in the row correspond to representative examples of: all explant stained with H&E (4×), 40× images of hydrogels stained with the Van Gieson's method and immunohistochemical using anti-CD31 for endothelial detection (40×). Black arrows indicate vessels with luminal erythrocytes. n = 6.

configuration), mechanical properties are mostly related to the number of covalent cross-links, intricate level of the network and molecular weight distribution, and not to physical crosslinking associated to the nature of the amino acid sequence of the gelatin source. In this context, physical crosslinking generated by electrostatic-derived helical arrangement of gelatin polypeptides [14] would be impeded to occur after photo-induction conducted at 40 °C due to mobility constraints imposed by the previously formed inter- and intra-polypeptide covalent crosslinks while the polypeptides were still under random coil configuration.

Interestingly, and associated to this last concept, the NMR relaxation time analysis on hydrogels (see Fig. 2a) effectively showed higher molecular mobility of hydrogels derived from salmon GelMA compared to bovine GelMA, although the hydrogels' macro-mechanical behavior measured by DMA and mechanical testing did not show differences between salmon and bovine sources of gelatin. The differences in NMR relaxation behavior could be explained by the level of mobility of the polypeptide chains in between zones of covalent inter- and intra-chain crosslinking, mobility that is directly associated to the presence or not of certain amino acids in the sequence that confers more rigidity to the polypeptide, such as proline and hydroxyproline (see bovine and salmon gelatin amino acid composition in Table S1). Thus, similar macro-mechanical behavior is mostly explained by the density of covalent crosslinks.

In a consecutive experiment, hydrogels fabricated with salmon GelMA and bovine GelMA were submitted to 2 h of incubation at 4 °C prior to photo-crosslinking at 4 °C and compared to hydrogels photo-crosslinked without pre-cooling and photo-crosslinked at 40 °C. Pre-cooling generated a tertiary structure conformational transformation from random coil to triple helix state, also denominated as physical crosslinking or gelation, and subsequently the photo-induction chemically fixed that configuration through a network of covalent bonds. Therefore, both physical crosslinking (triple helices) and covalent photo-crosslinking contributed to the increased mechanical properties of these pre-cooled hydrogels. In the case of salmon GelMA the pre-cooling-derived increment was significantly lower than Bovine GelMA (Fig. 1c), suggesting that the cold-adaptation reflected in the amino acid sequence of SG may be less prone to thermally-induced random coil to triple helix transformation upon cooling. This is also observed in the CD experiments (Fig. S6), in which the change in magnitude of the positive peak at 220 nm and a negative peak at 200 nm after isothermal incubation at 4 °C was remarkably greater for BG than SG.

Furthermore, a good correlation between the NMR transverse relaxation results and the pore sizes of hydrogels was observed. Lower molecular rigidity of hydrogels derived from functionalized SG, evidenced by the NMR relaxation time, can explain the larger pore sizes generated in SG-derived hydrogels after freeze-drying in comparison to hydrogels from functionalized BG. The pore expanding pressure provoke during water crystallization [60] and sublimation of ice water within the hydrogels may produce larger pore sizes in hydrogels derived from SG due to the increased molecular flexibility of the interconnected network of crosslinked gelatin polymers, whereas the higher molecular rigidity in hydrogels derived from BG imposes a stronger physical constraint to pore expansion. This presents an advantage for SG in the development of porous scaffold with improved post-cell seeding and better distribution of cells across the scaffold.

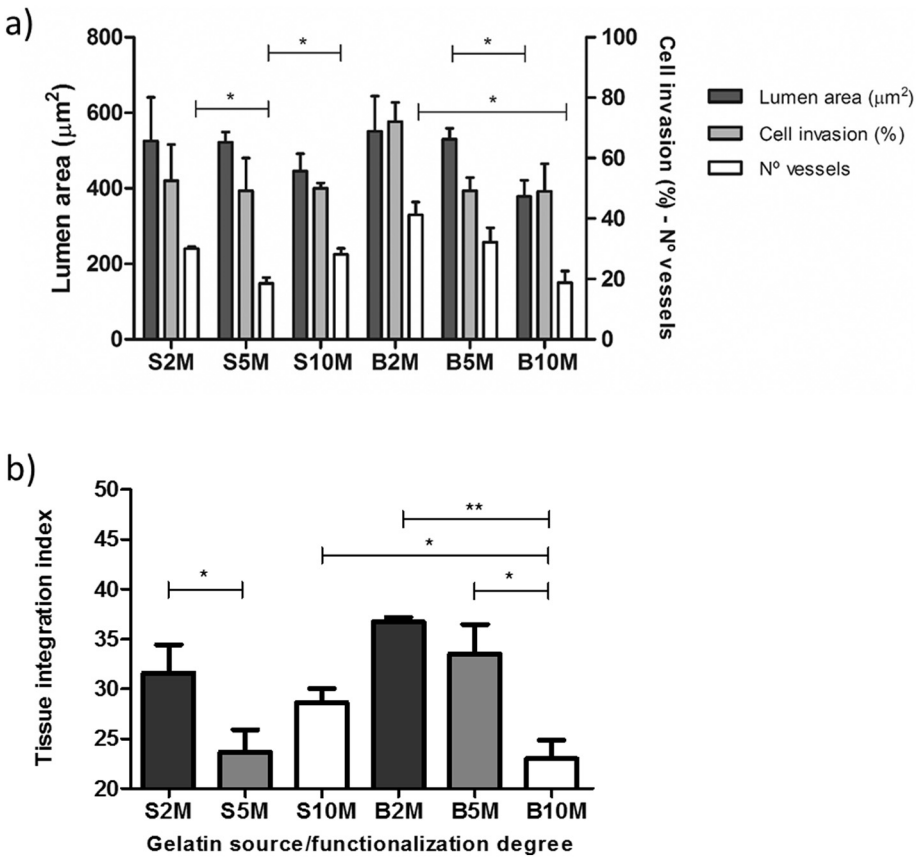

Fig. 8. Quantification of tissue integration. a) Quantification of vessel number per hydrogel (VN), percentage of cell repopulation or invasion (CI) and vessel luminal area (LA). b) Tissue integration scoring for each modified gelatin-derived hydrogel (CI × VN × LA). All analysis were performed using paraffined hydrogel sections from a transversal cut of the hydrogel disc at the middle distant between the bottom and top face of the implants. n = 6. Error bars = S.E. $p < 0.05$ = *; $p < 0.01$ = ** (Mann-Whitney test).

Having comparatively elucidated some of the macro and molecular behavior of hydrogels derived from salmon GelMA, several questions arise concerning the advantages of these characteristics in the biological spectra of tissue engineering. For example, one could speculate that larger molecular mobility of polypeptides is an advantage for faster cell-triggered scaffold remodeling *via* enzymatic hydrolysis, and faster invasion of cells and vascularization could be attained.

As mentioned previously, ECM-remodeling and vascularization is mediated by enzymatic action of cell-secreted metalloproteinases. For this family of hydrolases, catalytic activity relies on substrate flexibility for efficient bending at the enzymatic active site [26]. EC3.4/EC3.5 hydrolases become more efficient with increasing substrate flexibility, whereas for rigid and larger peptide/protein substrates, the number of freely rotatable bonds are restricted, stabilizing the reactant state of the substrate and limiting the product formation [26].

Conceptually, this was tested in this work measuring the enzymatic parameters (K_m and k_{cat}) of a collagenase using as substrate, a solution of SG or BG at different temperatures. These data (Fig. 4) allow for calculation of the activation energy, which is interpreted as the dependency of the enzymatic reaction on enthalpy (temperature) that permits the necessary molecular mobility for the reaction to occur. As expected, the cold-adapted gelatin showed an advantage in terms of the enzymatic efficiency and activation energy compared to BG. To extrapolate this information into the context of enzymatic hydrolysis of a hydrogel derived from functionalized and crosslinked gelatin, catalytic turnover of collagenase in the presence of hydrogels was measured, and comparison between the different gelatin sources at different level of functionalization was performed (Fig. 5 and Fig. S7). These experiments were conducted at 37 °C, since the study targets applications in the context of tissue engineering in humans. Interestingly, collagenase activity over hydrogels derived from salmon GelMA showed improved rate of catalysis, which was more evident as the degree of functionalization was higher. In this sense, it is expected that remodelling of ECM and cell invasion would be more efficient when SG-derived hydrogels are used in tissue engineering applications.

To prove this, an additional *in vitro* assay was conducted, in which remodeling of ECM and cell invasion was indirectly quantified by measuring the number of cells that are capable of transmigrating across a hydrogel fabricated on the topside of the porous Boyden chamber membrane (Fig. 6). Beside the expected negative correlation between remodeling of ECM/cell invasion and the degree of functionalization, surprisingly, migration of cells across hydrogels derived from functionalized BG was significantly higher than migration of cells in hydrogels based on functionalized SG. This observation disagrees with the results of hydrogel hydrolysis using collagenase (see Figs. 4 and 5), however the proteases responsible for the remodelling of ECM during cell migration and cell invasion are different from collagenase type 2, which is a more general protease with broader scope of substrate. Therefore, we can speculate that human metalloproteinases have higher specificity of substrate for BG than SG, probably due to the closer distance of evolution between human and bovine species, compared to human and salmon. Alternatively, bone marrow derived MSCs (BM-MSCs) could secrete metalloproteinases types prompted to more efficiently hydrolyze BG instead of SG.

There are > 25 described metalloproteinases that could be involved in cell invasion, vascularization and tissue regeneration, which can be distinctively secreted by different cell types involved in these biological processes. Therefore, the multi-cell dependent remodeling of ECM profile *in vivo* could still be different from the observed *in vitro* since BM-MSCs were the only cell type tested. In this regard, it was worthwhile evaluating the performance of cell-induced degradation of the hydrogel *in vivo* with a subcutaneous implantation model (Fig. S9). *In vivo* results show that salmon GelMA at lower degree of functionalization was fully remodeled and exhibited tissue integration after 14 days, corroborated the series of *in vitro* experimental evidences describing functionalized SG as a biomaterial with higher rate of degradation and advantages in relation to tissue engineering applications that require biomaterials with these characteristics.

Evaluation of the performance of cell invasion and vascularization in the different hydrogels *in vivo* after subcutaneous implantation was conducted (Figs. 7 and 8). Tissue integration of the hydrogels after 3 weeks subcutaneous implantation were evaluated through measurements of the level of cell-repopulation and vascularization. In line with previous *in vitro* experiments, the results established that a lower degree of functionalization resulted in better, and we hypothesise, faster integration of tissue (Figs. 7 and 8). Significant differences at lower degree of gelatin functionalization were not observed between the two sources of gelatin, however, for gelatin at 80% functionalized lysine, results showed that bovine gelatin outcompeted salmon gelatin at the same level of functionalization. Interestingly, at the higher degree of functionalization (~90%), while bovine GelMA and salmon GelMA are showing similar higher stiffness and crosslinking reactivity, salmon GelMA presented better tissue integration. In this case, this result is well reflected in the *in vitro* experiment of the enzymatic hydrolysis of the hydrogels (Fig. 5), showing a remarkable increase in the catalytic efficiency of collagenase on hydrogel fabricated with highly methacrylated salmon gelatin in comparison to hydrogels fabricated with bovine GelMA at the same degree of functionalization.

5. Conclusion

In this study, the technical advantages of a cold-adapted gelatin source for use in biofabrication purposes over a warm-adapted gelatin source was revealed comparing both their structural and molecular features. It was also demonstrated that SG-based hydrogels have a higher molecular flexibility compared to BG-based hydrogels, presenting an important advantage for tuning the rate of ECM remodeling. This could be the key characteristic for the improved integration and regeneration of tissue using biomaterials´ scaffolds. The biological responses may involve metalloproteinases and other relevant factors for the processes of tissue repair and regeneration and, most importantly, demonstrates the relevance of considering a salmon GelMA as a novel and biologically tolerable biomaterial when designing hydrogels for new applications in the field of regenerative medicine.

Abbreviations

GelMA	methacrylamide gelatin
PBS	phosphate buffer saline
ECM	extracellular matrix

Author contributions

The manuscript was written through contributions of all authors. All authors have given approval to the final version of the manuscript.

Funding sources

This work was supported by CORFO Chile (Corporación de Fomento a la Producción), through its grant 15CONTEC-47942 and by the Ministry of Education, Government of Chile through its grant UAN1301.

Notes

The authors declare no competing financial interest, excepting for M.K. and J.P.A. who received stipendium from Cells for Cells.

Appendix A. Supplementary data

Supporting tables and figures are included in this document.

- Analysis of amino acid composition for BG and SG, and GelMA versions at different degree of functionalization.
- SDS-PAGE of SG and BG polypeptides. And comparative quantification of primary amine groups in SG and BG using the OPA assay.
- ^{1}H NMR spectra for BG and SG, and GelMA versions at different degree of functionalization.
- *Z*-potential curves for BG and SG, and GelMA versions at different degree of functionalization.
- DSC evaluations using concentration and degree of functionalization as variables in SG and the GelMA version.
- Circular dichroism experiments for BG and SG, and GelMA versions at high degree of functionalization.
- Hydrogels hydrolysis evaluation using 50 U/ml of collagenase type 2.

Supplementary data to this article can be found online at https://doi.org/10.1016/j.msec.2019.04.020.

References

[1] E.S. Place, J.H. George, C.K. Williams, M.M. Stevens, Synthetic polymer scaffolds for tissue engineering, Chem. Soc. Rev. 38 (2009) 1139, https://doi.org/10.1039/b811392k.

[2] K.A. Rocco, M.W. Maxfield, C.A. Best, E.W. Dean, C.K. Breuer, In vivo applications of electrospun tissue-engineered vascular grafts: a review, Tissue Eng. B. Rev. 20 (2014) 628–640, https://doi.org/10.1089/ten.TEB.2014.0123.

[3] J. Kundu, J.H. Shim, J. Jang, S.W. Kim, D.W. Cho, An additive manufacturing-based PCL-alginate-chondrocyte bioprinted scaffold for cartilage tissue engineering, J. Tissue Eng. Regen. Med. (2013), https://doi.org/10.1002/term.1682.

[4] K. Algarrahi, D. Franck, C.E. Ghezzi, V. Cristofaro, X. Yang, M.P. Sullivan, Y.G. Chung, S. Affas, R. Jennings, D.L. Kaplan, C.R. Estrada, J.R. Mauney, J.R. Mauney, Acellular bi-layer silk fibroin scaffolds support functional tissue regeneration in a rat model of onlay esophagoplasty, Biomaterials 53 (2015) 149–159, https://doi.org/10.1016/j.biomaterials.2015.02.092.

[5] B.M. Baker, R.P. Shah, A.M. Silverstein, J.L. Esterhai, J.A. Burdick, R.L. Mauck, Sacrificial nanofibrous composites provide instruction without impediment and enable functional tissue formation, Proc. Natl. Acad. Sci. U. S. A. 109 (2012) 14176–14181, https://doi.org/10.1073/pnas.1206962109.

[6] M.A. Woodruff, C. Lange, F. Chen, P. Fratzl, D.W. Hutmacher, Nano- to macroscale remodeling of functional tissue-engineered bone, Adv. Healthc. Mater. 2 (2013) 546–551, https://doi.org/10.1002/adhm.201200289.

[7] P. Lu, K. Takai, V.M. Weaver, Z. Werb, Extracellular matrix degradation and remodeling in development and disease, Cold Spring Harb. Perspect. Biol. 3 (2011) a005058, https://doi.org/10.1101/cshperspect.a005058.

[8] S.B. Anderson, C.-C. Lin, D.V. Kuntzler, K.S. Anseth, The performance of human mesenchymal stem cells encapsulated in cell-degradable polymer-peptide hydrogels, Biomaterials 32 (2011) 3564–3574, https://doi.org/10.1016/j.biomaterials.2011.01.064.

[9] P.S. Briquez, L.E. Clegg, M.M. Martino, F. Mac Gabhann, J.A. Hubbell, Design principles for therapeutic angiogenic materials, Nat. Rev. Mater. 1 (2016) 15006, https://doi.org/10.1038/natrevmats.2015.6.

[10] S. Allazetta, T.C. Hausherr, M.P. Lutolf, Microfluidic synthesis of cell-type-specific artificial extracellular matrix hydrogels, Biomacromolecules 14 (2013) 1122–1131, https://doi.org/10.1021/bm4000162.

[11] K.B. Fonseca, D.B. Gomes, K. Lee, S.G. Santos, A. Sousa, E.A. Silva, D.J. Mooney, P.L. Granja, C.C. Barrias, Injectable MMP-sensitive alginate hydrogels as hMSC delivery systems, Biomacromolecules 15 (2014) 380–390, https://doi.org/10.1021/bm4016495.

[12] Y. Li, J. Rodrigues, H. Tomás, Injectable and biodegradable hydrogels: gelation, biodegradation and biomedical applications, Chem. Soc. Rev. 41 (2012) 2193–2221, https://doi.org/10.1039/C1CS15203C.

[13] Y. Liu, M.B. Chan-Park, A biomimetic hydrogel based on methacrylated dextran-graft-lysine and gelatin for 3D smooth muscle cell culture, Biomaterials 31 (2010) 1158–1170, https://doi.org/10.1016/j.biomaterials.2009.10.040.

[14] Liang Guo, Ralph H. Colby, Charles P. Lusignan, T.H. Whitesides, Kinetics of Triple Helix Formation in Semidilute Gelatin Solutions, (2003), https://doi.org/10.1021/MA034264S.

[15] K. Yue, G. Trujillo-de Santiago, M.M. Alvarez, A. Tamayol, N. Annabi, A. Khademhosseini, Synthesis, properties, and biomedical applications of gelatin methacryloyl (GelMA) hydrogels, Biomaterials 73 (2015) 254–271, https://doi.org/10.1016/j.biomaterials.2015.08.045.

[16] D. Loessner, C. Meinert, E. Kaemmerer, L.C. Martine, K. Yue, P.A. Levett, T.J. Klein, F.P.W. Melchels, A. Khademhosseini, D.W. Hutmacher, Functionalization, preparation and use of cell-laden gelatin methacryloyl-based hydrogels as modular tissue culture platforms, Nat. Protoc. 11 (2016) 727–746, https://doi.org/10.1038/nprot.2016.037.

[17] J.W. Nichol, S.T. Koshy, H. Bae, C.M. Hwang, S. Yamanlar, A. Khademhosseini, Cell-laden microengineered gelatin methacrylate hydrogels, Biomaterials 31 (2010) 5536–5544, https://doi.org/10.1016/j.biomaterials.2010.03.064.

[18] D.N. Heo, W.-K. Ko, M.S. Bae, J.B. Lee, D.-W. Lee, W. Byun, C.H. Lee, E.-C. Kim, B.-Y. Jung, I.K. Kwon, Enhanced bone regeneration with a gold nanoparticle–hydrogel complex, J. Mater. Chem. B 2 (2014) 1584–1593, https://doi.org/10.1039/C3TB21246G.

[19] X. Zhao, Q. Lang, L. Yildirimer, Z.Y. Lin, W. Cui, N. Annabi, K.W. Ng, M.R. Dokmeci, A.M. Ghaemmaghami, A. Khademhosseini, Photocrosslinkable gelatin hydrogel for epidermal tissue engineering, Adv. Healthc. Mater. 5 (2016) 108–118, https://doi.org/10.1002/adhm.201500005.

[20] S. Yunoki, K. Mori, T. Suzuki, N. Nagai, M. Munekata, Novel elastic material from collagen for tissue engineering, J. Mater. Sci. Mater. Med. 18 (2007) 1369–1375, https://doi.org/10.1007/s10856-007-0121-6.

[21] N. Nagai, R. Kubota, R. Okahashi, M. Munekata, Blood compatibility evaluation of elastic gelatin gel from salmon collagen, J. Biosci. Bioeng. 106 (2008) 412–415, https://doi.org/10.1263/jbb.106.412.

[22] H.J. Yoon, S.R. Shin, J.M. Cha, S.-H. Lee, J.-H. Kim, J.T. Do, H. Song, H. Bae, Cold water fish gelatin methacryloyl hydrogel for tissue engineering application, PLoS One 11 (2016) e0163902, , https://doi.org/10.1371/journal.pone.0163902.

[23] A.A. Karim, R. Bhat, Gelatin alternatives for the food industry: recent developments, challenges and prospects, Trends Food Sci. Technol. 19 (2008) 644–656, https://doi.org/10.1016/J.TIFS.2008.08.001.

[24] Christine Joly-Duhamel, and Dominique Hellio, M. Djabourov*, All gelatin networks: 1. Biodiversity and physical chemistry. Langmuir, (2002). doi:https://doi.org/10.1021/LA020189N.

[25] P. Díaz, D. López, S. Matiacevich, F. Osorio, J. Enrione, State diagram of salmon (Salmo salar) gelatin films, J. Sci. Food Agric. 91 (2011) 2558–2565, https://doi.org/10.1002/jsfa.4451.

[26] S.F. Sousa, M.J. Ramos, C. Lim, P.A. Fernandes, Relationship between enzyme/substrate properties and enzyme efficiency in hydrolases, ACS Catal. 5 (2015) 5877–5887, https://doi.org/10.1021/acscatal.5b00923.

[27] L. Demetrius, Role of enzyme–substrate flexibility in catalytic activity: an evolutionary perspective, J. Theor. Biol. 194 (1998) 175–194, https://doi.org/10.1006/JTBI.1998.0748.

[28] A.I. Van Den Bulcke, B. Bogdanov, N. De Rooze, E.H. Schacht, M. Cornelissen, H. Berghmans, Structural and rheological properties of methacrylamide modified gelatin hydrogels, Biomacromolecules 1 (2000) 31–38 http://www.ncbi.nlm.nih.gov/pubmed/11709840 , Accessed date: 23 August 2015.

[29] P.S.L. Janssen, J.W. van Nispen, P.A.T.A. Melgers, H.W.M. van den Bogaart, R.L.A.E. Hamelinck, B.C. Goverde, HPLC analysis of phenylthiocarbamyl (PTC) amino acids. I. Evaluation and optimization of the procedure, Chromatographia 22 (1986) 345–350, https://doi.org/10.1007/BF02268788.

[30] R. Rebane, K. Herodes, A sensitive method for free amino acids analysis by liquid chromatography with ultraviolet and mass spectrometric detection using pre-column derivatization with diethyl ethoxymethylenemalonate: application to the honey analysis, Anal. Chim. Acta 672 (2010) 79–84, https://doi.org/10.1016/j.aca.2010.04.014.

[31] K. Weber, M. Osborn, The reliability of molecular weight determinations by dodecyl sulfate-polyacrylamide gel electrophoresis, J. Biol. Chem. 244 (1969) 4406–4412 http://www.ncbi.nlm.nih.gov/pubmed/5806584 , Accessed date: 28 May 2018.

[32] P.M. Nielsen, D. Petersen, C. Dambmann, Improved method for determining food protein degree of hydrolysis, J. Food Sci. 66 (2001) 642–646, https://doi.org/10.1111/j.1365-2621.2001.tb04614.x.

[33] K. Yue, X. Li, K. Schrobback, A. Sheikhi, N. Annabi, J. Leijten, W. Zhang, Y.S. Zhang, D.W. Hutmacher, T.J. Klein, A. Khademhosseini, Structural analysis of photocrosslinkable methacryloyl-modified protein derivatives, Biomaterials 139 (2017) 163–171, https://doi.org/10.1016/j.biomaterials.2017.04.050.

[34] E. Hoch, C. Schuh, T. Hirth, G.E.M. Tovar, K. Borchers, Stiff gelatin hydrogels can be photo-chemically synthesized from low viscous gelatin solutions using molecularly functionalized gelatin with a high degree of methacrylation, J. Mater. Sci. Mater. Med. 23 (2012) 2607–2617, https://doi.org/10.1007/s10856-012-4731-2.

[35] P. Díaz-Calderón, L. Caballero, F. Melo, J. Enrione, Molecular configuration of gelatin–water suspensions at low concentration, Food Hydrocoll. 39 (2014) 171–179, https://doi.org/10.1016/J.FOODHYD.2013.12.019.

[36] J.R. Tumbleston, D. Shirvanyants, N. Ermoshkin, R. Januszewicz, A.R. Johnson, D. Kelly, K. Chen, R. Pinschmidt, J.P. Rolland, A. Ermoshkin, E.T. Samulski, J.M. DeSimone, Additive manufacturing. Continuous liquid interface production of 3D objects, Science 347 (2015) 1349–1352, https://doi.org/10.1126/science.aaa2397.

[37] C.D. O'Connell, B. Zhang, C. Onofrillo, S. Duchi, R. Blanchard, A. Quigley, J. Bourke, S. Gambhir, R. Kapsa, C. Di Bella, P. Choong, G.G. Wallace, Tailoring the mechanical properties of gelatin methacryloyl hydrogels through manipulation of the photocrosslinking conditions, Soft Matter 14 (2018) 2142–2151, https://doi.org/10.1039/C7SM02187A.

[38] J.W. Heyt, M.J. Diaz, Pressure drop in flat-oval spiral air duct, ASHRAE Trans. 81 (1975) 221–232.

[39] W.N. Nowak, H. Taha, N. Kachamakova-Trojanowska, J. Stępniewski, J.A. Markiewicz, A. Kusienicka, K. Szade, A. Szade, K. Bukowska-Strakova, K. Hajduk, D. Klóska, A. Kopacz, A. Grochot-Przęczek, K. Barthenheier, C. Cauvin, J. Dulak, A. Józkowicz, Murine bone marrow mesenchymal stromal cells respond efficiently to oxidative stress despite the low level of heme oxygenases 1 and 2, Antioxid. Redox Signal. (2018), https://doi.org/10.1089/ars.2017.7097 ars.2017.7097.

[40] E. Dernbach, C. Urbich, R.P. Brandes, W.K. Hofmann, A.M. Zeiher, S. Dimmeler, Y. Fujita, S. Kothari, R. Mohle, L.R. Sauvage, M.A. Moore, R.F. Storb, W.P. Hammond, Antioxidative stress-associated genes in circulating progenitor cells: evidence for enhanced resistance against oxidative stress, Blood 104 (2004) 3591–3597, https://doi.org/10.1182/blood-2003-12-4103.

[41] M.J. Rutten, B. Laraway, C.R. Gregory, H. Xie, C. Renken, C. Keese, K.W. Gregory,

Rapid assay of stem cell functionality and potency using electric cell-substrate impedance sensing, Stem Cell Res Ther 6 (2015) 192, , https://doi.org/10.1186/s13287-015-0182-2.
[42] C.R. Justus, N. Leffler, M. Ruiz-Echevarria, L.V. Yang, In vitro cell migration and invasion assays, J. Vis. Exp. (2014) e51046, https://doi.org/10.3791/51046.
[43] M. Campos-Mora, R.A. Morales, F. Pérez, T. Gajardo, J. Campos, D. Catalan, J.C. Aguillón, K. Pino-Lagos, Neuropilin-1^{+} regulatory T cells promote skin allograft survival and modulate effector CD4^{+} T cells phenotypic signature, Immunol. Cell Biol. 93 (2015) 113–119, https://doi.org/10.1038/icb.2014.77.
[44] J. Van Hoorick, P. Gruber, M. Markovic, M. Tromayer, J. Van Erps, H. Thienpont, R. Liska, A. Ovsianikov, P. Dubruel, S. Van Vlierberghe, Cross-linkable gelatins with superior mechanical properties through carboxylic acid modification: increasing the two-photon polymerization potential, Biomacromolecules 18 (2017) 3260–3272, https://doi.org/10.1021/acs.biomac.7b00905.
[45] C. Claaßen, M.H. Claaßen, V. Truffault, L. Sewald, G.E.M. Tovar, K. Borchers, A. Southan, Quantification of substitution of gelatin methacryloyl: best practice and current pitfalls, Biomacromolecules 19 (2018) 42–52, https://doi.org/10.1021/acs.biomac.7b01221.
[46] William T. Brinkman, Karthik Nagapudi, Benjamin S. Thomas, Elliot L. Chaikof, Photo-cross-linking of type I collagen gels in the presence of smooth muscle cells: mechanical properties, cell viability, and function, Biomacromelcules (2003), https://doi.org/10.1021/BM0257412.
[47] B. Lee, N. Lum, L. Seow, P. Lim, L. Tan, Synthesis and characterization of types A and B gelatin methacryloyl for bioink applications, Materials (Basel) 9 (2016) 797, https://doi.org/10.3390/ma9100797.
[48] M.D. Shoulders, R.T. Raines, Collagen structure and stability, Annu. Rev. Biochem. 78 (2009) 929–958, https://doi.org/10.1146/annurev.biochem.77.032207.120833.
[49] A.V. Persikov, J.A.M. Ramshaw, A. Kirkpatrick, B. Brodsky, Electrostatic interactions involving lysine make major contributions to collagen triple-helix stability, Biochemistry 44 (2005) 1414–1422, https://doi.org/10.1021/bi048216r.
[50] A. Adams, Analysis of solid technical polymers by compact NMR, TrAC Trends Anal. Chem. 83 (2016) 107–119, https://doi.org/10.1016/J.TRAC.2016.04.003.
[51] N.J. Greenfield, Analysis of the kinetics of folding of proteins and peptides using circular dichroism, Nat. Protoc. 1 (2007) 2891–2899, https://doi.org/10.1038/nprot.2006.244.
[52] J.L.S. Lopes, A.J. Miles, L. Whitmore, B.A. Wallace, Distinct circular dichroism spectroscopic signatures of polyproline II and unordered secondary structures: applications in secondary structure analyses, Protein Sci. 23 (2014) 1765–1772, https://doi.org/10.1002/pro.2558.
[53] Y.-C. Chen, R.-Z. Lin, H. Qi, Y. Yang, H. Bae, J.M. Melero-Martin, A. Khademhosseini, Functional human vascular network generated in photocrosslinkable gelatin methacrylate hydrogels, Adv. Funct. Mater. 22 (2012) 2027–2039, https://doi.org/10.1002/adfm.201101662.
[54] J.A. Benton, C.A. DeForest, V. Vivekanandan, K.S. Anseth, Photocrosslinking of gelatin macromers to synthesize porous hydrogels that promote valvular interstitial cell function, Tissue Eng. A 15 (2009) 3221–3230, https://doi.org/10.1089/ten.TEA.2008.0545.
[55] I. Noshadi, S. Hong, K.E. Sullivan, E. Shirzaei Sani, R. Portillo-Lara, A. Tamayol, S.R. Shin, A.E. Gao, W.L. Stoppel, L.D. Black III, A. Khademhosseini, N. Annabi, In vitro and in vivo analysis of visible light crosslinkable gelatin methacryloyl (GelMA) hydrogels, Biomater. Sci. 5 (2017) 2093–2105, https://doi.org/10.1039/C7BM00110J.
[56] P.S. Low, J.L. Bada, G.N. Somero, Temperature adaptation of enzymes: roles of the free energy, the enthalpy, and the entropy of activation, Proc. Natl. Acad. Sci. U. S. A. 70 (1973) 430–432 http://www.ncbi.nlm.nih.gov/pubmed/4510286 , Accessed date: 28 May 2018.
[57] T. Lonhienne, C. Gerday, G. Feller, Psychrophilic enzymes: revisiting the thermodynamic parameters of activation may explain local flexibility, Biochim. Biophys. Acta 1543 (2000) 1–10 http://www.ncbi.nlm.nih.gov/pubmed/11087936 , Accessed date: 28 May 2018.
[58] M. Sirova, S. Van Vlierberghe, V. Matyasova, P. Rossmann, E. Schacht, P. Dubruel, B. Rihova, Immunocompatibility evaluation of hydrogel-coated polyimide implants for applications in regenerative medicine, J. Biomed. Mater. Res. A 102 (2014) 1982–1990, https://doi.org/10.1002/jbm.a.34873.
[59] T. Billiet, E. Gevaert, T. De Schryver, M. Cornelissen, P. Dubruel, The 3D printing of gelatin methacrylamide cell-laden tissue-engineered constructs with high cell viability, Biomaterials 35 (2014) 49–62, https://doi.org/10.1016/j.biomaterials.2013.09.078.
[60] J. Desarnaud, D. Bonn, N. Shahidzadeh, The pressure induced by salt crystallization in confinement, Sci. Rep. 6 (2016) 30856, , https://doi.org/10.1038/srep30856.